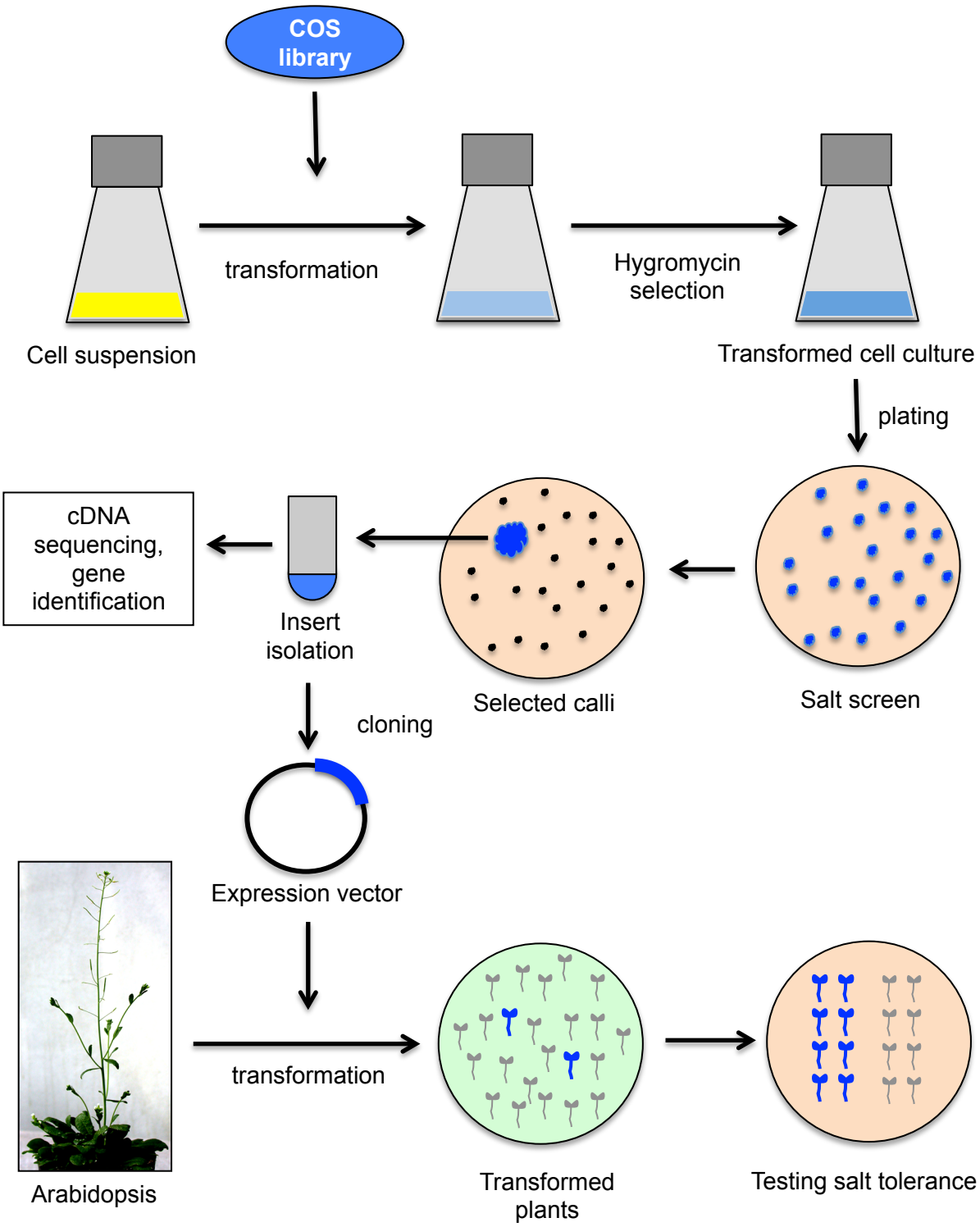

Figure S1. Schematic illustration of COS screening and cloning strategy.
Arabidopsis cell suspension was transformed with the COS cDNA library. Salt tolerant calli were selected in the presence of 5mM estradiol and used for DNA isolation and identification of cDNAs carried by the COS expression vector T-DNA insertions. The identified HSFA4A cDNA was cloned into a plant expression vector pER8GW, and transformed into Arabidopsis to verify its capacity to improve stress tolerance in plants.

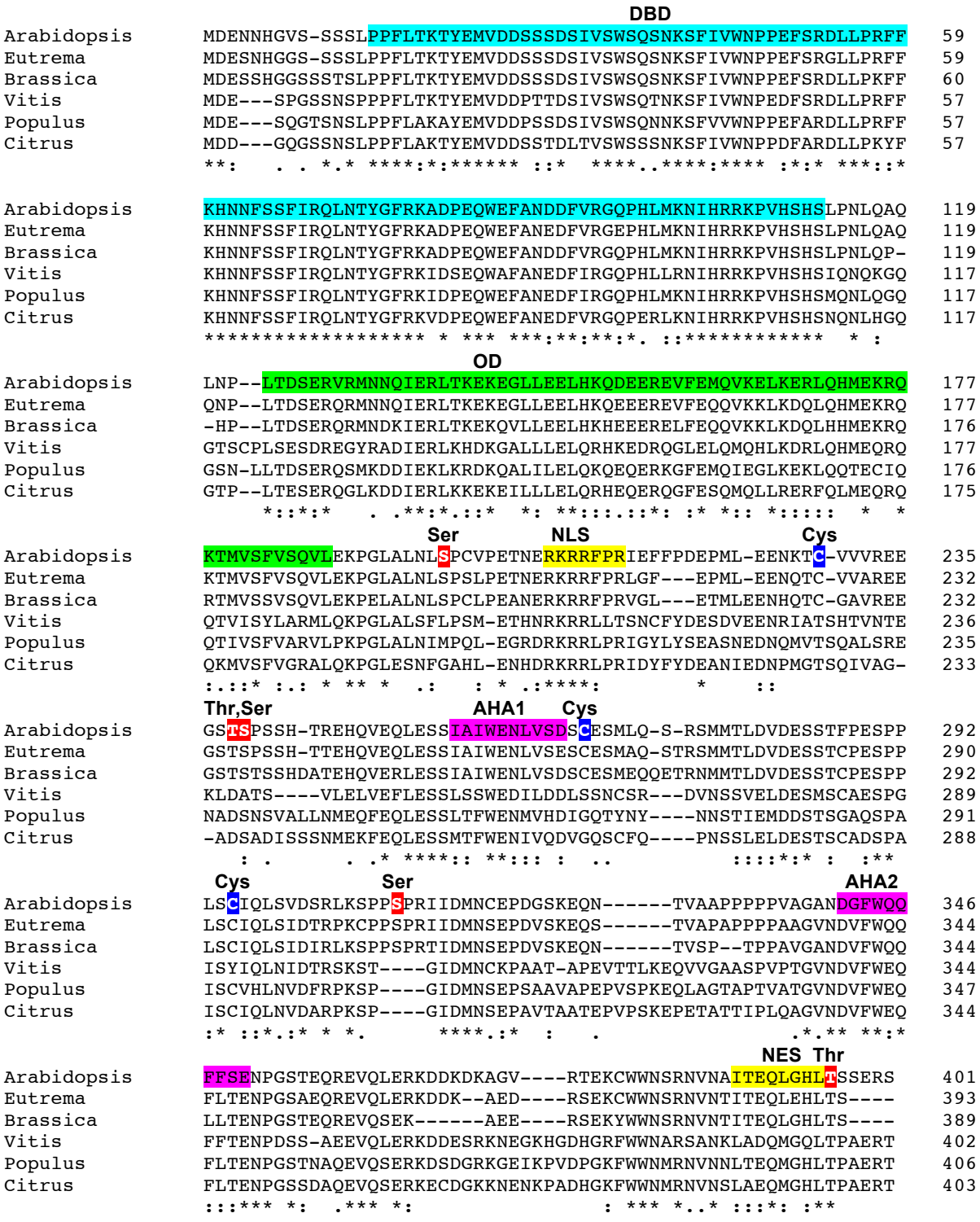

DBD DNA binding doman, **OD** HR-A/HR-B oligomerization domain, **NLS**, **NES** nuclear localization, **AHA** activator motifs, (Nover et al., 2001),

C Cys residues conserved in Brassicaeae, **S,T** phosphorylated Ser or Thr residues (MS data).

Figure S2. Multiple sequence alignment of six HSFA4A protein sequences. CLUSTAL O(1.2.0) multiple sequence alignment was made with the following sequences: *Arabidopsis thaliana* (AEE84101), *Eutrema salsugineum* (*Thellungiella salsuginea*, ESQ55497), *Brassica napus* (ADX69244), *Vitis vinifera* (XP_002267171), *Populus trichocarpa* (EEE97421), *Citrus sinensis* (XP_006467594). Domain structure of the Arabidopsis HSFA4A is indicated according to Nover et al., (2001) Cell Stress Chaperones 6: 177-189.

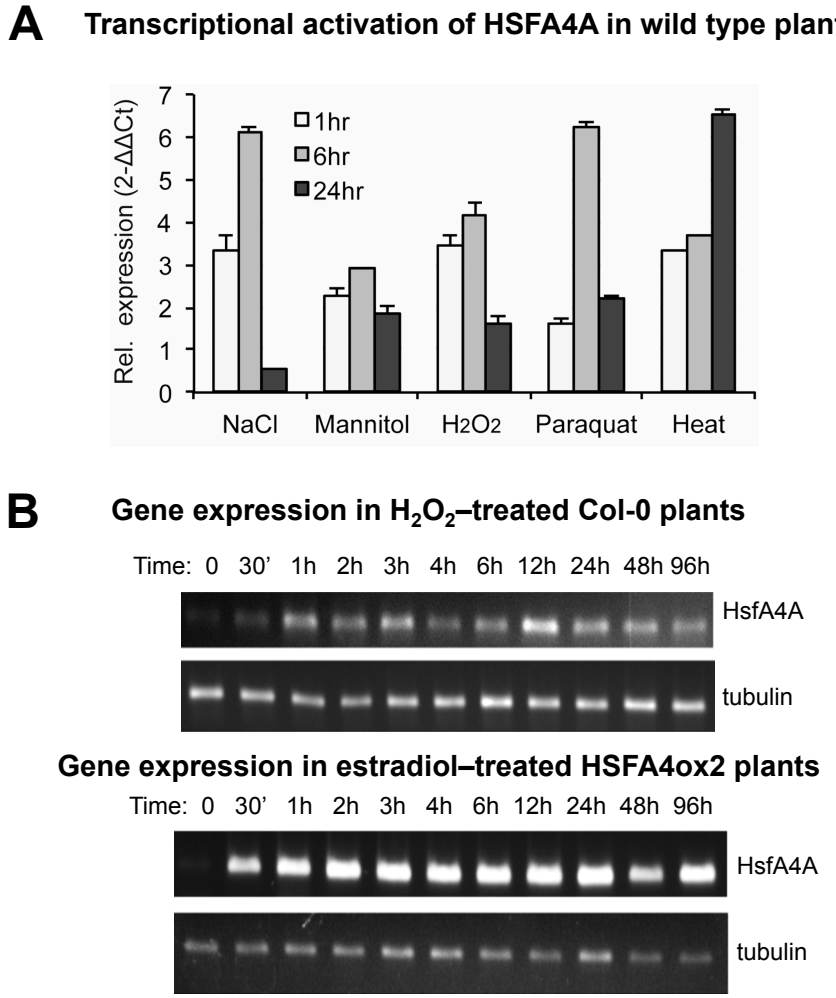

Figure S3. Regulation of HSFA4A transcription. A) Transcriptional activation of *HSFA4A* by salt (150 mM NaCl), osmotic (300 mM mannitol), oxidative (1 mM H_2O_2, 1 µM paraquat) and heat (37°C) stress in wild type plants. One relative unit corresponds to the transcript level of non-treated plants at the first time points of measurements. Bars indicate standard deviation. B) Induction of the *HSFA4A* gene in wild-type plants by 1 mM H_2O_2. C) Induction of *HSFA4A* in transgenic Arabidopsis plants (HSF4ox2 line) by 5 µM estradiol. Reference gene: β-tubulin (*AT5G62690*)

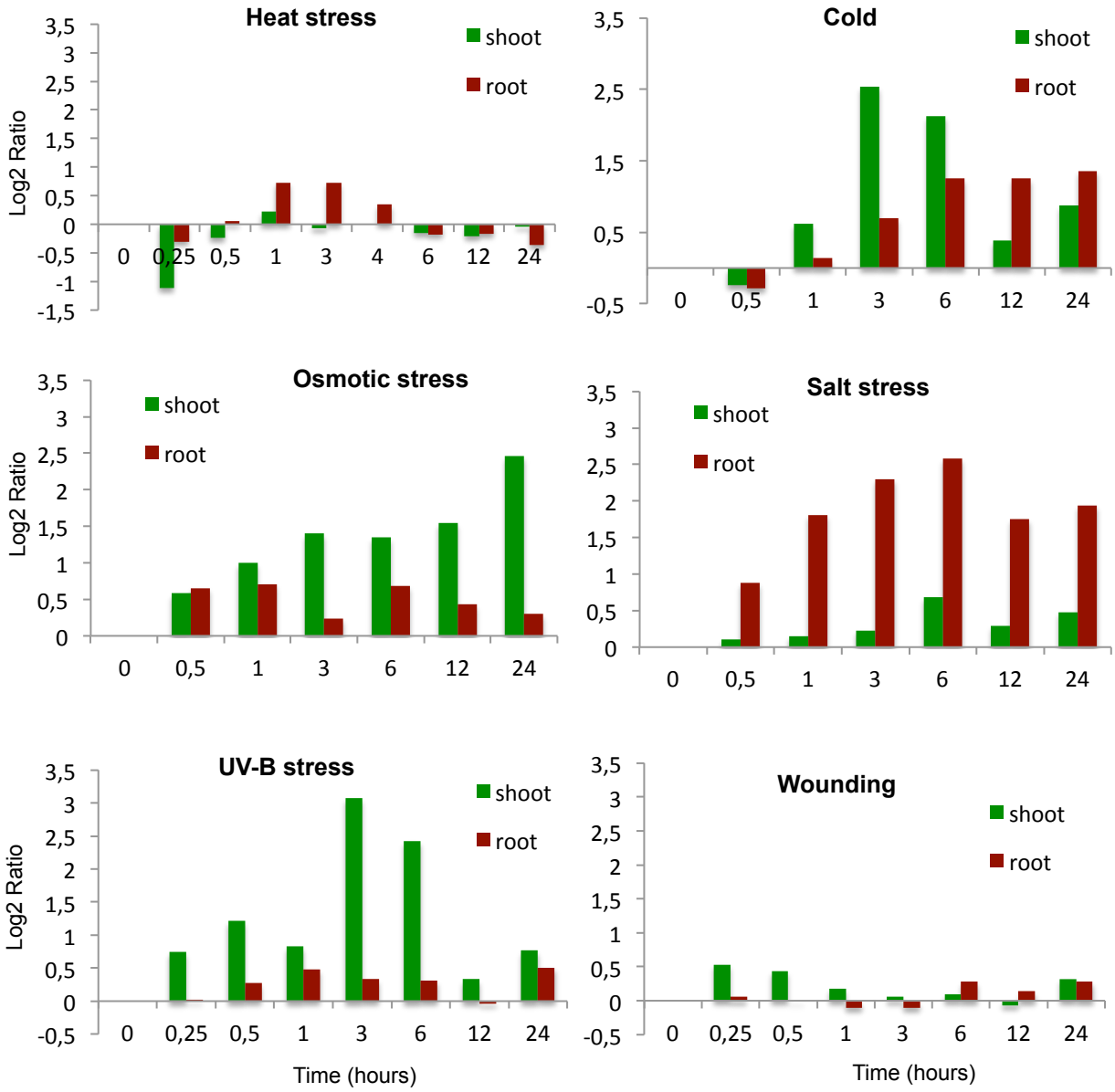

Figure S4. Transcriptional activation of HSFA4A gene in different abiotic stress conditions. Data were extracted from from public transcript database eFP Browser (http://bar.utoronto.ca/efp_arabidopsis). Numerical data were processed and diagrams were prepared with Microsoft Excel.

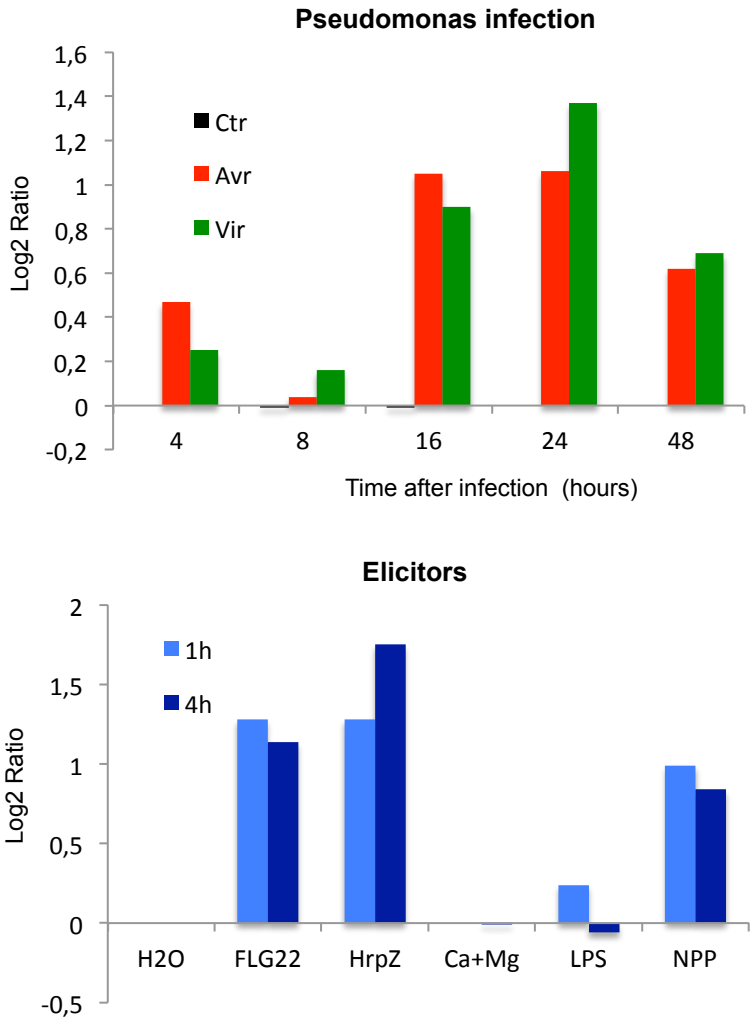

Figure S5. Transcriptional activation of HSFA4A gene by biotic stress. Effect of bacterial infection (Pseudomonas) and by bacterial (FLG22, HrpZ) and fungal (NPP) effectors on HSFA4A expression. Data were extracted from from public transcript database eFP Browser (http://bar.utoronto.ca/efp_arabidopsis). Numerical data were processed and diagrams were prepared with Microsoft Excel.

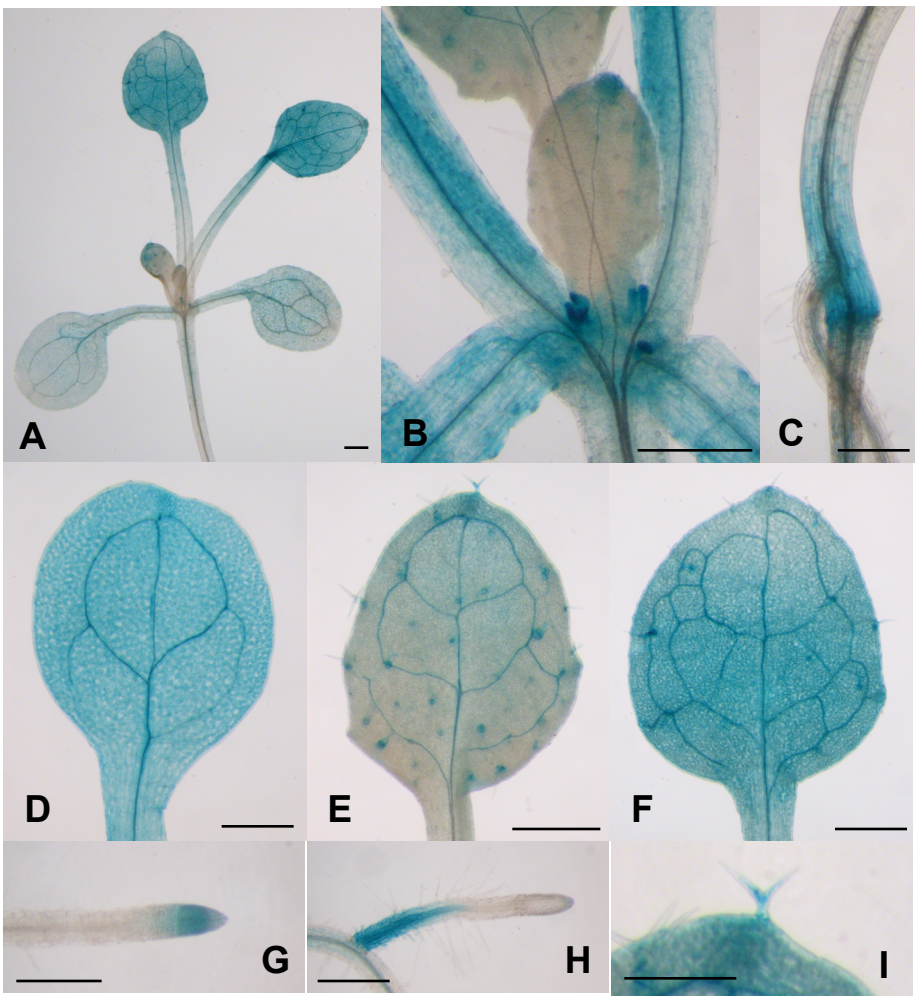

Figure S6. Spatial expression of pHSFA4A-GUS in transgenic plants. GUS activity was monitored by histochemical staining in 12 days-old Arabidopsis plants and are shown in whole seedlings (A), the shoot tip region (B), hypocotyl and root junction (C), cotyledons (D), young leaves (E), mature leaves (F), root tips (G), lateral roots (H) and trichomes (I). Bars indicate 0.5mm.

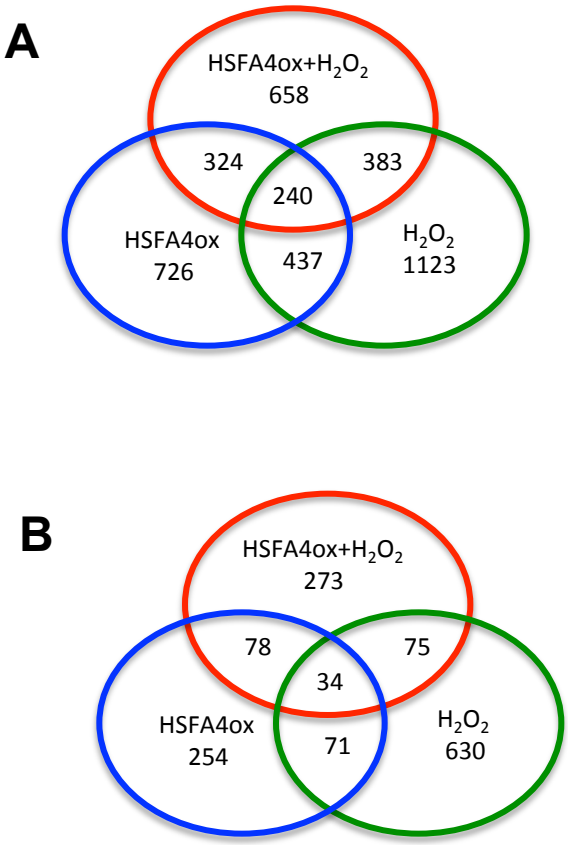

Figure S7. HSFA4A regulates the expression of a large set of genes. RNA-Seq transcript profiling was performed to identify possible transcriptional targets of HSFA4A in relation to oxidative stress. Col-0 and HSFA4Aox2 plants were treated with 5 µM estradiol in the absence or presence of 1 mM H_2O_2. Venn diagrams depicting the distribution of Arabidopsis genes that upregulated (**A**) or downregulated (**B**) at least two times compared to Col-0. **H_2O_2:** Col-0+H_2O_2 vs Col-0; **HSFA4ox:** HSFA4ox2 vs Col-0 and **HSFA4ox+H_2O_2**: HSFA4ox2+ H_2O_2 vs Col-0.

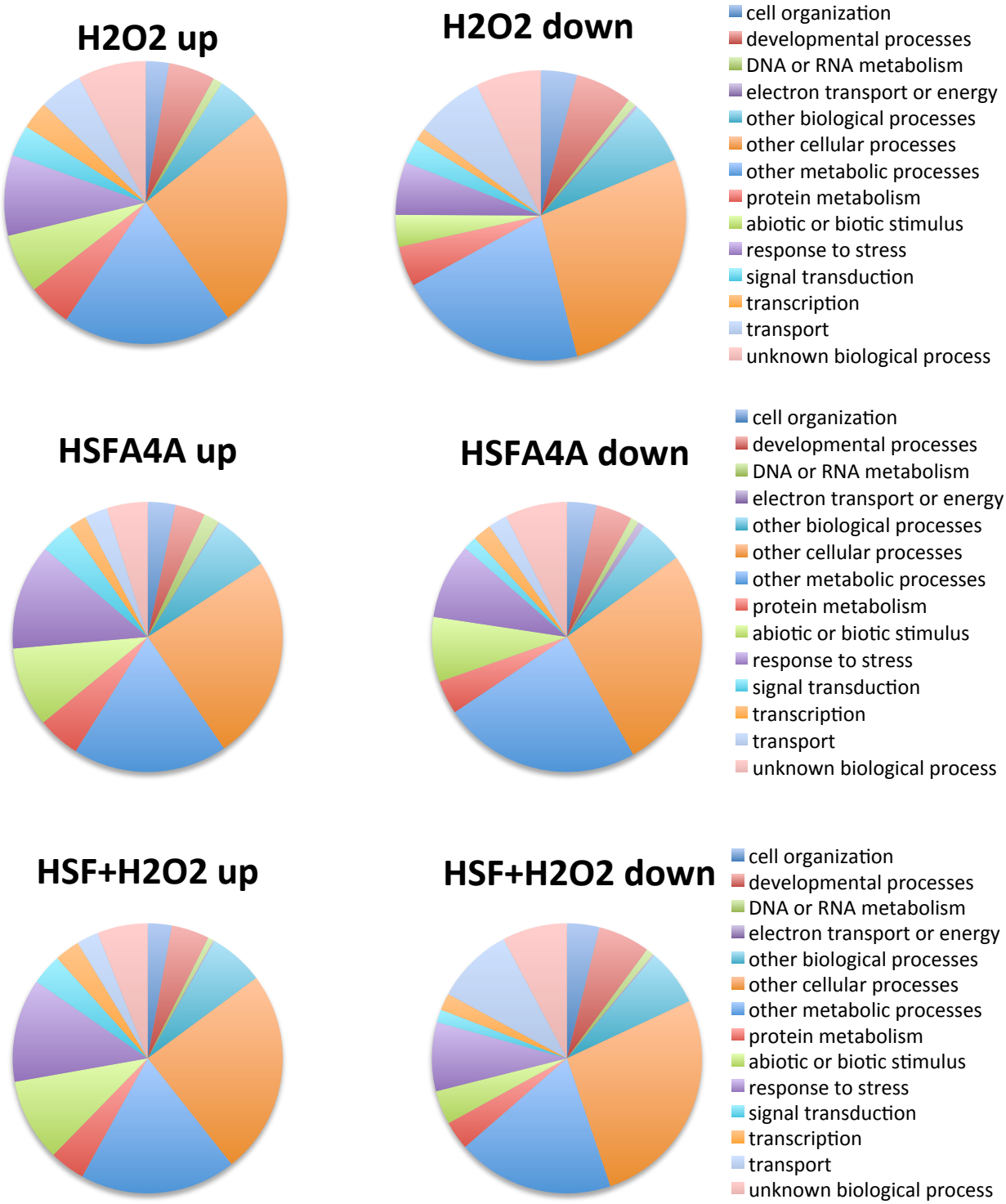

Figure S8A. Gene Ontology categorization (Biological Process) of gene sets which were up or downregulated by hydrogen peroxide in Col-0 plants (H2O2 up and H2O2 down) or in HSFA4Aox2 versus Col-0 plants (HSFA4A up and HSFA4A down, respectively) or by hydrogen peroxide in HSFA4Aox2 plants (HSF+H2O2 up and HSF+H2O2 down, respectively). Data were obtained from RNAseq transcript profiling experiment, GO categories were set up by Bulk Retrieval function of the TAIR web site (www.arabidopsis.org) and processed with MS Excel. Note, that genes involved in abiotic or biotic stimulus and response to stress are more frequent in categories induced by hydrogen peroxide, HSFA4A overexpression or by hydrogen peroxide in HSFA4Aox plants versus those downregulated by these conditions.

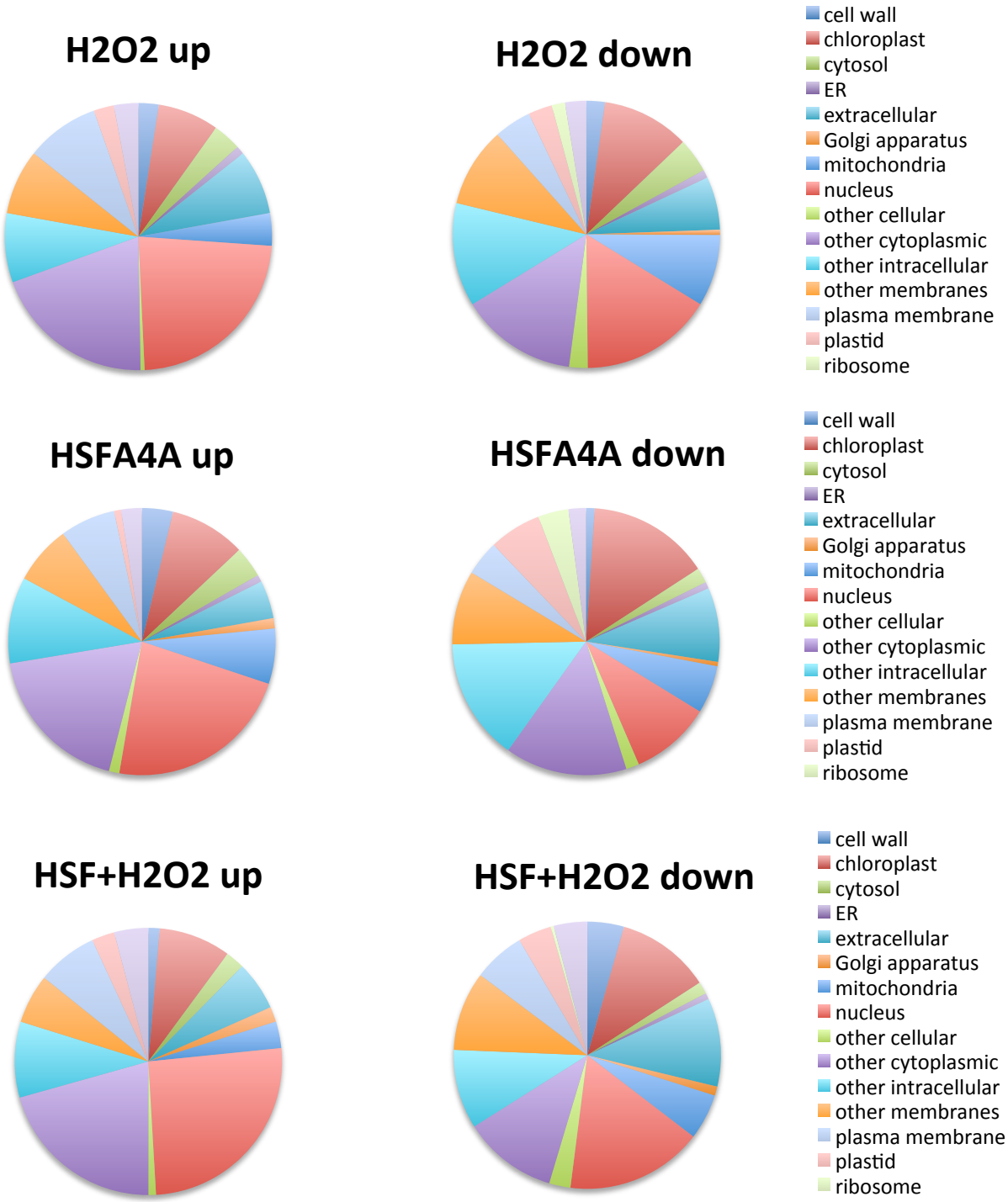

Figure S8B. Gene Ontology categorization (Cellular Component) of gene sets which were up or downregulated by hydrogen peroxide in Col-0 plants (H2O2 up and H2O2 down) or in HSFA4Aox2 versus Col-0 plants (HSFA4A up and HSFA4A down, respectively) or by hydrogen peroxide in HSFA4Aox2 plants (HSF+H2O2 up and HSF+H2O2 down, respectively). Data were obtained from RNAseq transcript profiling experiment, GO categories were set up by Bulk Retrieval function of the TAIR web site (www.arabidopsis.org) and processed with MS Excel. Note, that the category of nuclear localization is larger among genes upregulated by HSFA4Aox when compared to downregulated genes.

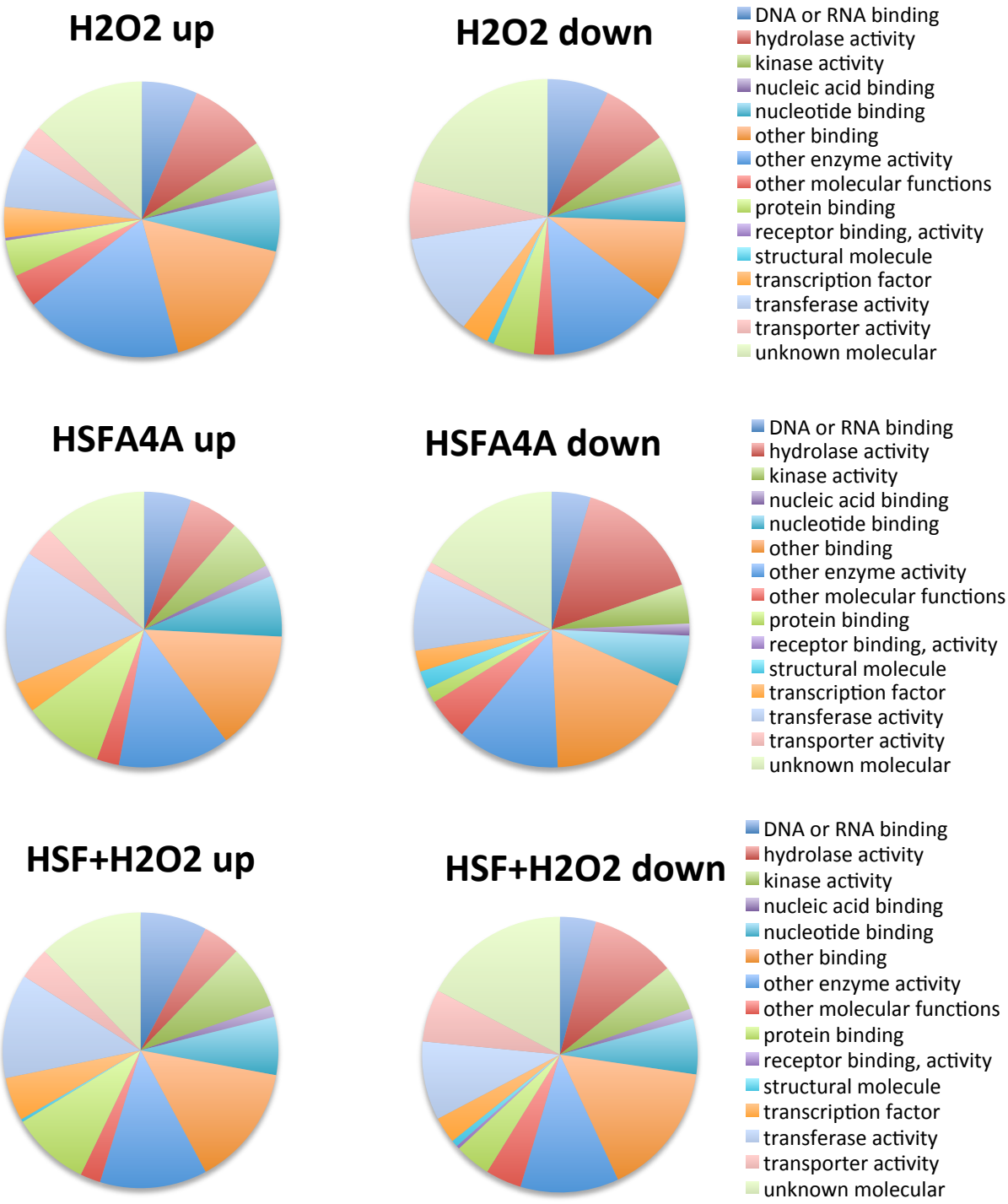

Figure S8C. Gene Ontology categorization (Molecular Function) of gene sets which were up or downregulated by hydrogen peroxide in Col-0 plants (H2O2 up and H2O2 down) or in HSFA4Aox2 versus Col-0 plants (HSFA4A up and HSFA4A down, respectively) or by hydrogen peroxide in HSFA4Aox2 plants (HSF+H2O2 up and HSF+H2O2 down, respectively). Data were obtained from RNAseq transcript profiling experiment, GO categories were set up by Bulk Retrieval function of the TAIR web site (www.arabidopsis.org) and processed with MS Excel. Note, that the category protein binding is larger among genes upregulated by HSFA4Aox, while the category DNA or RNA binding is larger among genes upregulated by HSFA4Aox with H2O2 treatment versus downregulated ones in these conditions.

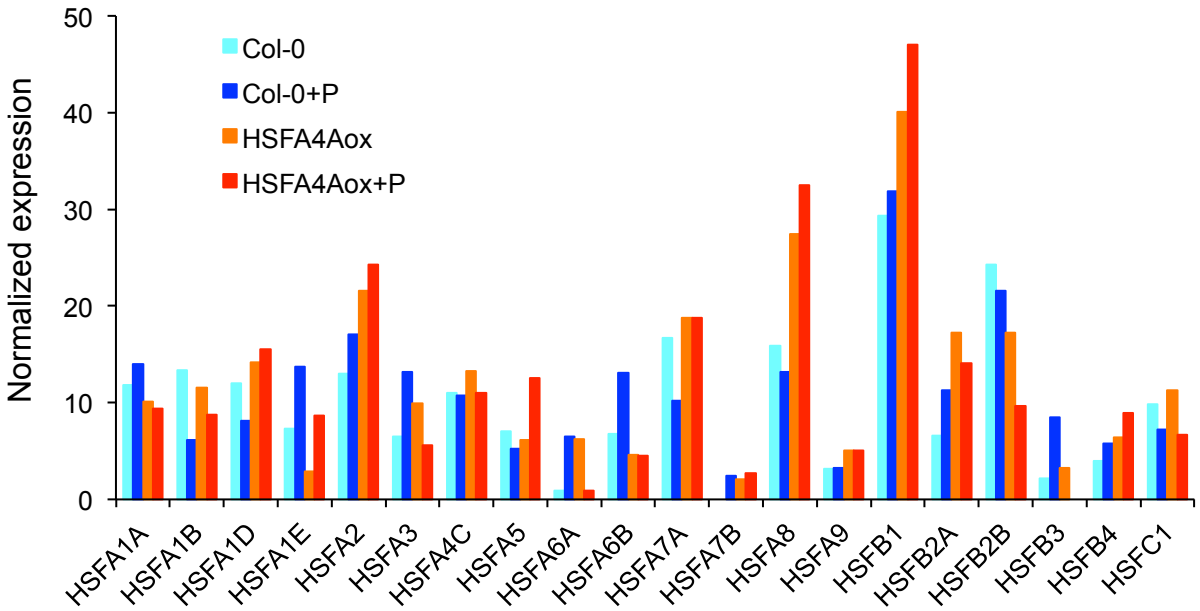

Figure S9. Expression profiles of Arabidopsis heat shock factors in wild type and HSFA4A overexpressing plants. Expression data from transcript profiling experiment were assembled. Samples: Col-0 (untreated wild type), Col-0+P (hydrogen peroxide-treated wild type), HSFA4Aox (untreated HSFA4A overexpressing), HSFA4Aox+P (hydrogen peroxide-treated HSFA4A overexpressing), all samples were treated with estradiol.

Supplemental Tables

Table S1. Summary of results of cell suspension transformation with the COS library.

Experiment	No. of colonies	Selected microcalli	Calli with sustained growth
1	500000	93	2
2	540000	119	2
3	190000	79	0
all	**1230000**	**291**	**4**

Table S2. Arabidopsis cDNAs identified in COS-transformed cell cultures showing enhanced growth on high salt medium.

Callus no.	Fragment size	AGI	Encoded protein	Inserted cDNA
1.1	1,9kb	*AT4G18880*	Heat shock transcription factor A4A	Full length
1.2	1,4kb	*AT3G44300*	Nitrilase 2	Full length
7.1	0,8kb	*AT5G48810*	Cytocrome b5 B	Full length
7.2	1,0kb	*AT1G44900*	Minichromosome maintenance 2	Truncated
9	0,5kb	*AT3G48580*	Xyloglucan endotransglucosylase 11	Truncated
14	0,8kb	*AT2G30860*	Glutathione S-transferase 9	Full length

Table S3. Genes upregulated by both HSFA4A overexpression and H_2O_2 treatment.

AGI	Protein	HSFA4A	H_2O_2	HSFA4A +H_2O_2	HSE	Other TF
AT5G12030	small heat shock protein HSP17.6A	7,3	16,1	22,3	0	AP2/EREBP, MYB, C2C2(Zn) Dof
AT5G12020	small heat shock protein HSP17.6II	5,3	4,5	18,3	1	AP2/EREBP
AT1G64500	glutaredoxin-like protein	2,9	4,6	15,3	1	HD-HOX
AT3G46230	small heat shock protein HSP17.4	4,7	3,3	14,5	1	HSFB, C2C2(Zn) Dof
AT1G53540	HSP20-like chaperone protein	5,6	5,2	12,4	2	HSFB, HD-HOX
AT4G22960	Protein of unknown function (DUF544)	6,6	13,8	12,4	1	C2C2(Zn) Dof
AT1G17010	2-oxoglutarate and Fe(II)-dependent oxygenase	7,3	4,3	12,3	0	
AT1G69570	Dof-type zinc finger DNA-binding protein	3,2	4,3	11,1	1	bZIP, MYB, GATA
AT1G16030	heat shock protein HSP70B	2,9	7,5	8,6	0	HSFB
AT4G25200	small heat shock protein, HSP23.6-MITO	11,3	1,4	8,2	1	MYB
AT1G06160	ethylene response factor, ERF094, ORA59	2,7	2,1	6,9	1	AP2/EREBP, MYB, SBP,
AT5G27420	E3 ubiquitin-protein ligase, ATL31, CNI1,	5,1	4,2	6,8	1	bZIP, Trihelix, HD-HOX, C2C2(Zn) Dof
AT2G30770	Cytochrome P450 protein, CYP71A13	5,1	6,0	5,7	0	HD-HOX, TBP
AT3G15450	Aluminium induced, YGL and LRDR protein	2,3	1,8	5,7	0	Trihelix, MYB
AT3G28210	stress-associated protein 12, SAP12, PMZ	3,0	1,7	5,3	0	HSFB
AT1G71000	Chaperone DnaJ-domain protein;	3,5	2,6	4,8	1	AP2/EREBP, MYB, HD-HOX,
AT5G52640	heat shock protein, HSP90.1	5,1	1,5	4,3	2	AP2/EREBP, MYB, HD-HOX,
AT5G44310	Late embryogenesis abundant (LEA) protein	2,2	5,2	4,3	1	HSFB, Dof
AT2G29500	HSP20-like chaperone protein	2,0	2,1	4,1	1	HD-HOX
AT4G23210	cysteine-rich receptor kinase 13, CRK13	2,3	2,2	3,9	0	AP2/EREBP, MYB
AT2G04040	MATE family transporter related protein TX1	2,3	2,3	3,7	1	HD-HOX, C2C2(Zn) Dof
AT1G32460	unknown protein	3,3	3,0	3,5	1	
AT1G74310	heat shock protein HSP101	2,4	2,1	3,4	1	bZIP, AP2/EREBP, HD-HOX
AT1G27730	salt tolerance zinc finger, STZ/ZAT10	1,7	3,0	3,2	0	HSFB, AP2/EREBP, MYB, HD-HOX
AT5G41750	Disease resistance protein (TIR-NBS-LRR)	1,6	1,4	3,0	2	MYB, HD-HOX, C2C2(Zn) Dof, CBF
AT5G48570	peptidylprolyl isomerase ROF2	3,0	1,9	2,8	1	MYB, HD-HOX, C2C2(Zn) Dof
AT5G25930	LRR-type protein kinase	2,4	1,4	2,8	0	MYB
AT1G29060	Target SNARE coiled-coil domain protein;	2,0	2,3	2,8	0	bZIP, MYB, HD-HOX
AT4G21400	cysteine-rich receptor kinase 28, CRK28	1,9	2,2	2,7	0	HSFB, MYB, HD-HOX
AT1G22510	unknown RING/U-box protein (DUF 1232)	2,7	3,1	2,7	0	bZIP, MYB
AT3G17611	rhomboid-like protein 14, RBL14	2,1	2,2	2,6	0	AP2/EREBP, Trihelix, MYB, TCP
AT5G46350	WRKY transcription factor 8, WRKY8	2,6	2,8	2,6	2	HSFB, Trihelix,
AT2G27490	dephospho-CoA kinase, ATCOAE	1,9	1,8	2,6	1	HSFB, AP2/EREBP, SBP, HD-HOX, C2C2(Zn) Dof
AT1G72920	Toll-Interleukin-Resistance (TIR) protein	3,7	2,3	2,5	0	Trihelix, HD-HOX, C2C2(Zn) Dof
AT5G04340	C2H2 zinc finger transcription factor, ZAT6	2,5	2,1	2,5	1	AP2/EREBP, Trihelix, MYB
AT1G08315	ARM repeat superfamily protein;	2,8	2,2	2,5	1	
AT2G47180	galactinol synthase 1, GolS1	2,5	2,0	2,5	1	AP2/EREBP, MYB, HD-HOX
AT3G43230	RING/FYVE/PHD-type zinc finger protein;	2,2	2,0	2,4	0	HSFB, AP2/EREBP
AT1G33030	O-methyltransferase family protein;	2,6	4,4	2,4	0	HSFB, AP2/EREBP, HD-HOX
AT5G52760	Copper transport protein family;	2,8	6,9	2,4	1	
AT2G31990	Exostosin family protein;	2,8	2,2	2,3	1	MYB, HD-HOX
AT5G61270	phytochrome-interacting factor 7, PIF7	1,6	1,9	2,3	0	MYB
AT1G26420	FAD-binding Berberine family protein;	2,6	2,0	2,3	1	AP2/EREBP, MYB

AT1G02560	ATP-dependent Clp protease, CLPP5	3,0	3,4	2,1	0	bZIP, HD-KNOTTED, Trihelix
						HSFB, C2H2(Zn), Trihelix, HD-HOX,
AT2G29990	alternative NAD(P)H dehydrogenase 2, NDA2	1,8	2,1	2,1	2	CBF, HD-ZIP
AT1G68570	Major facilitator superfamily protein;	2,2	2,1	2,1	1	MADS, MYB,
AT2G43580	Chitinase family protein;	3,2	6,0	2,1	1	
AT1G60730	NAD(P)-linked oxidoreductase protein;	2,4	2,0	2,0	1	HD-HOX
AT4G18250	putative receptor serine/threonine kinase	2,8	1,9	1,9	0	Trihelix, HD-HOX
AT4G28020	unknown protein;	2,6	1,9	1,9	0	AP2/EREBP, MYB, HD-HOX
AT3G03440	ARM repeat protein	2,6	1,9	1,9	0	MYB
AT2G41640	Glycosyltransferase family 61 protein	2,6	1,9	1,9	1	MYB, HD-HOX
AT5G17370	Transducin/WD40 repeat-like protein	2,8	1,9	1,9	0	HD-HOX
AT4G25390	putative protein kinase protein	2,1	3,9	1,8	0	MYB
AT2G14290	Protein of unknown function DUF295	2,4	4,7	1,8	0	MYB, ABI3/VP1
AT5G59820	C2H2-type zinc finger protein, ZAT12, RHL41	1,3	1,4	1,5	2	MYB
AT5G24110	WRKY transcription factor 30, WRKY30	3,4	3,7	0,5	2	ABI3/VP1, HD-HOX, MADS

List of genes found commonly upregulated by HSFA4A overexpression and H_2O_2 treatment. RNA-Seq was performed with RNA from two weeks old Col-0 and HSFa4A-ox2 plants after plus /minus 1mM H_2O_2 treatment. Plants for every sample were equally treated with 5 µM estradiol. Values indicate differential gene expression (fold change) relative to Col-0 minus H_2O_2 sample. Categories presented in columns: **AGI:** AGI number of genes. **Protein**: type of encoded protein, **HSFA4A:** fold change in HSFA4Aox2 minus H_2O_2 vs. Col-0 minus H_2O_2 samples. **H_2O_2:** fold change in Col-0 plus H_2O_2 vs. Col-0 minus H_2O_2 samples, **HSFA4A+H_2O_2**: fold change in HSFA4Aox2 plus H_2O_2 vs. Col-0 minus H_2O_2 samples, **HSE:** number of Heat Shock Elements identified in the 1000bp promoter regions determined with Promomer (bar.utoronto.ca). **Other TF** category indicate other predicted TF binding sites (AthaMap promoter search tool, www.athamap.de, 75% restriction).

According to Genevestigator (www.genevestigator.com) analysis of public transcript profiling data 80% of these genes are induced by several abiotic stresses (heat, ozone, UV light, hypoxia, osmotic and salt stress, H_2O_2), several pathogens (*P. syringe, B. graminis*), effectors (FLG22, HrpZ), in *cat2* and *flu* mutants, down-regulated during germination and by MeJA.

Table S4. Genes downregulated by both HSFA4A overexpression and H_2O_2 treatment.

AGI	Protein	HSFA4A	H_2O_2	HSFA4A +H_2O_2	HSE	Other TF
AT1G05250	peroxidase 1/2	-1,4	-4,3	-12,9	0	AP2/EREBP
AT4G30500	Protein of unknown function (DUF788);	-8,3	-5,3	-11,1	1	HD-HOX, MYB
AT4G02270	protein root hair specific 13, RHS13	-3,8	-4,0	-5,9	0	bZIP, MYB
AT2G13100	starvation-induced glycerol-3-phosphate permease	-5,1	-9,6	-5,2	0	MYB, HD-HOX
AT2G35810	unknown protein;	-2,7	-2,8	-5,1	0	HD-HOX, MYB
AT1G30870	peroxidase 7	-2,8	-2,4	-4,6	1	C2C2(Zn) Dof, HD-HOX, HD-ZIP
AT2G03420	unknown protein	-7,5	-2,2	-4,5	0	MYB, HD-HOX, C2C2(Zn) Dof
AT5G17820	peroxidase 57	-1,8	-2,0	-4,4	0	HD-HOX, MYB
AT1G48930	Glycosyl hydrolase 9C, endoglucanase 5, GH9C1	-1,6	-1,5	-4,3	0	AP2/EREBP, MYB, SBP
AT3G05950	RmlC-like cupins superfamily protein;	-2,2	-1,7	-3,4	0	TBP
AT4G01450	nodulin MtN21 /EamA-like transporter protein	-1,9	-1,8	-2,9	0	MYB
AT4G28040	nodulin MtN21 /EamA-like transporter protein	-1,8	-2,4	-2,7	0	AP2/EREBP, MYB, HD-ZIP
AT1G14345	NAD(P)-linked oxidoreductase superfamily protein	-8,2	-2,7	-2,6	0	bZIP, MYB
AT4G23270	cysteine-rich receptor-like protein kinase 19, CRK19	-2,4	-3,5	-2,5	0	HD-HOX
AT3G23800	selenium-binding protein 3, SBP3	-1,8	-1,8	-2,5	1	AP2/EREBP, MYB, HD-ZIP, MADS
AT5G44820	Nucleotide-diphospho-sugar transferase protein	-1,8	-4,1	-2,4	1	HSFB
AT5G59320	non-specific lipid-transfer protein 3, LTP3	-3,6	-2,2	-2,4	0	C2C2(Zn) Dof, TBP
AT4G30290	xyloglucan:xyloglucosyl transferase, XTH19	-2,7	-6,6	-2,4	2	HSFB
AT1G14960	major latex-related protein	-2,5	-2,1	-2,4	0	HD-ZIP
AT3G58100	Plasmodesmata callose-binding protein 5, PDCB5	-2,2	-2,0	-2,1	1	MYB, HD-HOX, bZIP
AT5G42180	peroxidase 64	-2,1	-1,9	-2,1	0	MYB
AT3G63110	IPT3, isopentenyltransferase 3	-2,2	-2,3	-2,0	0	ABI3/VP1, MYB, HD-HOX
AT4G30650	Low temperature and salt responsive protein	-4,3	-1,9	-2,0	0	AP2/EREBP, HD-HOX, MYB
AT5G22860	Serine carboxypeptidase S28 family protein;	-2,0	-2,6	-2,0	1	HD-HOX
AT5G64620	Cell wall/vacuolar inhibitor of fructosidase 2, C/VIF2	-3,2	-1,8	-1,9	0	HD-HOX, HD-ZIP
AT2G40080	Early flowering 4, ELF4	-2,5	-2,2	-1,9	0	HSFB
AT5G26260	TRAF-like family protein;	-2,0	-3,0	-1,9	0	
AT3G58990	isopropylmalate isomerase 1, IPMI1	-1,7	-2,7	-1,9	0	AP2/EREBP, MYB, HD-HOX
AT4G23690	Disease resistance-responsive (dirigent-like) protein	-2,8	-1,9	-1,8	1	HD-HOX, MYB, C2C2(Zn) Dof
AT1G53900	Eukaryotic translation initiation factor 2B (eIF-2B)	-1,8	-2,2	-1,8	0	HD-HOX
AT5G42250	Zinc-binding alcohol dehydrogenase family protein;	-2,2	-2,3	-1,8	3	MYB, HD-ZIP
AT3G21770	Peroxidase superfamily protein;	-1,8	-2,1	-1,8	0	
AT2G36485	ENTH/VHS family protein;	-1,8	-2,5	-1,8	0	AP2/EREBP, MYB, HD-HOX
AT4G30660	Low temperature and salt responsive protein	-2,1	-4,1	-1,8	1	HSFB, HD-HOX, HD-ZIP
AT3G03480	acetyl CoA:(Z)-3-hexen-1-ol acetyltransferase, CHAT	-2,3	-2,9	-1,7	0	AP2/EREBP, MYB, HD-HOX
AT5G50160	ferric reduction oxidase 8, FRO8	-2,4	-1,8	-1,7	0	AP2/EREBP, HD-HOX, MYB
AT3G25805	unknown protein	-2,3	-2,9	-1,7	0	AP2/EREBP
AT1G49720	ABA responsive element-binding factor 1, ABF1	-2,3	-2,0	-1,7	0	AP2/EREBP, GATA
AT2G25210	Ribosomal protein L39 family protein	-2,2	-2,5	-1,6	0	MYB
AT3G53190	Pectin lyase-like superfamily protein	-2,4	-1,7	-1,6	0	MYB
AT3G05880	Rare-cold-inducible 2A, RCI2A	-2,2	-3,2	-1,6	1	HD-HOX, MYB
AT2G21210	SAUR-like auxin-responsive protein	-3,0	-1,9	-1,6	0	TBP, MYB

List of genes found commonly downregulated by HSFA4A overexpression and H_2O_2 treatments. **Categories:** AGI, Protein, HSFA4A, H_2O_2, HSFA4A+H_2O_2, HSE and Other TF are the same as in Table S3. According to Genevestigator (www.genevestigator.com) data, 75% of these genes are downregulated by abiotic stresses (UV light, drought, osmotic, hypoxia, ozone), repressed by SA, and induced during germination.

Table S5. Occurrence of predicted transcription factor binding sites in promoter regions of HSFA4A and hydrogen peroxide induced or repressed genes (listed on tables S3 and S4). Bold letter indicate binding sites which were overrepresented in upregulated genes, while bold italics shows those which were more frequent in downregulated genes. Data were assembled using the Promomer (bar.utoronto.ca) and AthaMap promoter (www.athamap.de) search tools.

TF binding sites	% of sites in induced genes	% of sites in repressed genes
HSF	**70**	**33**
HSFB	**33**	**10**
Trihelix	**30**	**6**
MYC_MYB	**63**	**29**
ABI3/VP1	3	2
C2H2(Zn)	3	2
SBP	3	2
bZIP_DOF	103	69
LFY	33	27
C2C2(Zn) Dof	15	12
AP2/EREBP	55	49
HOX2a_HOX2a	115	110
HD-HOX	62	59
RAV	17	16
MYB	207	204
bZIP	27	27
TSS	100	102
GATA	15	16
GARP/ARR-B	10	12
CAMTA	3	4
WRKY(Zn)	23	29
MADS	***43***	***65***
C2C2(Zn) GATA	***8***	***24***
GRF	***3***	***10***
TBP	***2***	***6***
HD-ZIP	***2***	***16***
CBF	3	0
HD-KNOTTED	2	0
NAC	2	0
TCP	5	0

Table S6. List of oligonucleotides used in this study.

Code	5' - 3' sequence	Use	Reference
HsfA4A-seq2F	GCTTGCTTTGAACCTATCGCCG	HsfA4A (AT4G18880) cDNA sequencing	This study
HsfA4A-seq4F	GACGGATTCAGAACGAGTGAGAATG	HsfA4A (AT4G18880) cDNA sequencing	This study
HsfA4A-seqR	CACTCGTTCTGAATCCGTCA	HsfA4A (AT4G18880) cDNA sequencing	This study
HsfA4A-seq7R	GCGATAGGTTCAAAGCAAGC	HsfA4A (AT4G18880) cDNA sequencing	This study
hsfa4a_gen_F	CATTCCACCAAACCCAATCTTTGT	*hsfa4a* mutant gene-specific (genotyping)	This study
hsfa4a_gen_R	TTGGTGAGGAAAGGTGGAAGTG	*hsfa4a* mutant gene-specific (genotyping)	This study
HsfA4A-RT-F	CGAGCAACGGGAAGT TCAATTAGA	RT-PCR of HsfA4A gene	This study
HsfA4A-RT-R	CTGAACCATACCTAAGTACTGTAATCGAAAAC	RT-PCR of HsfA4A gene	This study
HsfA4A-qF	CTTTGAACCTATCGCCGTGT	HsfA4A (AT4G18880) Q-RTPCR	This study
HsfA4A-qR	TGTGTGTGAAGAAGGGCTTG	HsfA4A (AT4G18880) Q-RTPCR	This study
Hsf-prom-5(EcoRI):	TGACTGAATTCCCACATTCCACACTTGCCTTT	HsfA4A promoter cloning in pENTRY-BS (-)	This study
Hsf-prom-3(BamHI)_noATG	TGATTGGATCCCTCTGAAAACACTTTTAACAACTCTCACACTC	HsfA4A promoter cloning in pENTRY-BS (-)	This study
Hsf-prom-seq1F	AATTCGTCCTACTCCGACCA	HsfA4A promoter sequencing	This study
Hsf-prom-seq2F	TGATCCGACTTTTTCTTGCAC	HsfA4A promoter sequencing	This study
Hsf-prom-seq3F	ATCGTCGTCGTCGTAAATCC	HsfA4A promoter sequencing	This study
HsfA4A-5'(BamHI)	TGAGCGGATCCATGGATGAGAATAATCATGGAGTTTC	Cloning in pPCV-Y/CFP-H, pET28a, pMALC2, pGAD424, pGBT9	This study
HsfA4A-5'(Hind III)	TGAGCAAGCTTATGGATGAGAATAATCATGGAGTTTC	Cloning in pSAT1A, pPILY	This study
HsfA4A-3' (SmaI)_ noSTOP	TGATTCCCGGGACTTCTCTCTGAAGAAGTCAGAT	Cloning in pSAT1A, pPILY, pPCV-Y/CFP-H	This study
HsfA4A-3'(HindIII)	AAGCTTATCAACTTCTCTCTGAAGAAGTCAGAT	Cloning in pET28a, pMALC2	This study
HsfA4A-3'(SalI)	TGAGCGTCGACTCAACTTCTCTCTGAAGAAGTCAGAT	Cloning in pGAD424, pGBT9	This study
MPK3-5'(BamHI)	TGAGCGG ATC CAA ATGAACACCGGCGGTGGCCAATAC	Cloning in pET28c, pGAD424, pGBT9	This study
MPK6-5'(BamHI)	TGAGCGG ATC CTC ATGGACGGTGGTTCAGGTCAACCGGC	Cloning in pET28c, pGAD424, pGBT9	This study

MPK3-3'(SalI)	TGAGCGTCGACCTAACCGTATGTTGGATTGAGTGC	Cloning in pET28c, pGAD424, pGBT9	This study
MPK6-3'(SalI)	TGAGCGTCGACCTATTGCTGATATTCTGGATTGAAAG	Cloning in pET28c, pGAD424, pGBT9	This study
3'C229_Hsf_R	CCTTCCTCTCTCACAACAACAGCAGTTTTGTTCTCTTCCAACA	HsfA4A Site-directed mutagenesis, C229A	This study
3'C267_Hsf_R	GATTGTAACATACTCTCAGCAGAATCCGATACAAG	HsfA4A Site-directed mutagenesis, C267A	This study
3'C295_Hsf_R	GAATCGACACTTAACTGTATAGCAGAAAGAGGAGGGCTCTCTG	HsfA4A Site-directed mutagenesis, C295A	This study
Hsp17.6A-qF	CCAAAGAAAAAGCCAAGAAGC	Hsp17.6A gene (AT5G12030) quantitative PCR	This study
Hsp17.6A-qR	TGGAAACCTTCCAAACTCCA	Hsp17.6A gene (AT5G12030) quantitative PCR	This study
Zat6-qF	GTGACCTTGACCTGCCTTCTTC	Zat6 gene (AT5G04340) quantitative PCR	This study
Zat6-qR	CTCCGGCAGATTGAGTAAGC	Zat6 gene (AT5G04340) quantitative PCR	This study
Zat12-qF	GACGCTTTGTCGTCTGGATT	Zat12 gene (AT5G59820) quantitative PCR	This study
Zat12-qR	GTGTCCTCCCAAAGCTTGTC	Zat12 gene (AT5G59820) quantitative PCR	This study
Hsp90-qF	GTGGTTCCTTCACTGTCACTAG	Hsp90 gene (AT5G52640) quantitative PCR	This study
Hsp90-qR	TTCACCAAGTCTTTGAGTCTCC	Hsp90 gene (AT5G52640) quantitative PCR	This study
ER8A	GCTTGGGCTGCAGGTCGAGGCTAA	amplification of inserts in pER8 vector	Papdi et al., 2008
ER8B	CTGGTGTGTGGGCAATGAAACTGATGC	amplification of inserts in pER8 vector	Papdi et al., 2008
GAPDH2_qF	AATGGAAAATTGACCGGAATGT	GAPDH2 (AT1G13440) Q-RTPCR reference	Papdi et al., 2008
GAPDH2_qR	CGGTGAGATCAACAACTGAGACA	GAPDH2 (AT1G13440) Q-RTPCR reference	Papdi et al., 2008
Tubulin2-RT-F	AGGAACTGGATCTGGTATGGGAACAT	tubulin 2 (AT5G62690) Q-RTPCR reference	Koncz C.,
Tubulin2-RT-R	GTCACACCAGACATAGTAGCAGAAATCAAG	tubulin 2 (AT5G62690) Q-RTPCR reference	Koncz C.,
DONR1	TCGCGTTAACGCTAGCATGGATCTC	pDONR201 sequencing	Invitrogen
DONR2	GTAACATCAGAGATTTTGAGACAC	pDONR201 sequencing	Invitrogen
LB-4	CGTGTGCCAGGTGCCCACGGAATAGT	Left border T-DNA-specific (genotyping)	INRA
WRKY30-qF	AGAGCGATGATTCCGATCAAG	WRKY30 gene (AT5G24110) quantitative PCR	Besseau et al., 2012
WRKY30-qR	CATCGTCCAGCGTTCTATCAA	WRKY30 gene (AT5G24110) quantitative PCR	Besseau et al., 2012
PDC-qF	CGATTATGGCACTAACCGGATT	PDC1 gene (At4g33070) quantitative PCR	Banti et al., 2010

PDC-qR	TGTTCACCACCGCCTGATAAC	PDC1 gene (At4g33070) quantitative PCR	Banti et al., 2010
ADH-qF	GAATCGCTGGTGCTTCTAGG	ADH1 gene (At1g77120) quantitative PCR	Papdi et al., 2008
ADH-qR	CTCAGCGATCACCTGTTGAA	ADH1 gene (At1g77120) quantitative PCR	Papdi et al., 2008
3' S198A _Hsf_R	GGGAACACACGGAGCTAGGTTCAAAGC	HsfA4A Site-directed mutagenesis	This study
3' T238A _Hsf_R	TGAAGAAGGGCTAGCAGAACCTTCCTC	HsfA4A Site-directed mutagenesis	This study
3' S239A _Hsf_R	GTGTGAAGAAGGAGCTGTAGAACCTTC	HsfA4A Site-directed mutagenesis	This study
5' S309A _Hsf_F	CAAATCTCCTCCTGCTCCAAGGATCATC	HsfA4A Site-directed mutagenesis	This study
3' T396A _Hsf_R-HindIII	AGTCAAAGCTTATCAACTTCTCTCTGAAGAAGCCAGATGTCCAAG	HsfA4A Site-directed mutagenesis	This study
5' Hsp-prom_EcoRI	TGACTGAATTCCGGACTGTTCCAAATTTCCT	Hsp17.6A promoter cloning in pPCV-LUC+	This study
3' Hsp-prom_SalI	TGATTGTCGACTCTTAGCTGTTGTGTTAACTTCC	Hsp17.6A promoter cloning in pPCV-LUC+	This study

References:

Besseau S, Li J, Palva ET (2012) WRKY54 and WRKY70 co-operate as negative regulators of leaf senescence in Arabidopsis thaliana. J Exp Bot 63, 2667–2679

Papdi, C., Abraham, E., Joseph, M.P., Popescu, C., Koncz, C., Szabados, L. (2008). Functional identification of Arabidopsis stress regulatory genes using the controlled cDNA overexpression system. Plant Physiol 147, 528-542.

Banti V, Mafessoni F, Loreti E, Alpi A, Perata P. (2010). The heat-inducible transcription factor HsfA2 enhances anoxia tolerance in Arabidopsis. Plant Physiol. 152(3):1471-83.

Phospho-Ser198. **Corresponding phosphopeptide represents [179-207] of HSFA4A (Uniprot ID:O49403)**

TMVSFVSQVLEKPGLALNLS(Phospho)PC(Carbamidomethyl)VPETNER^{+3}

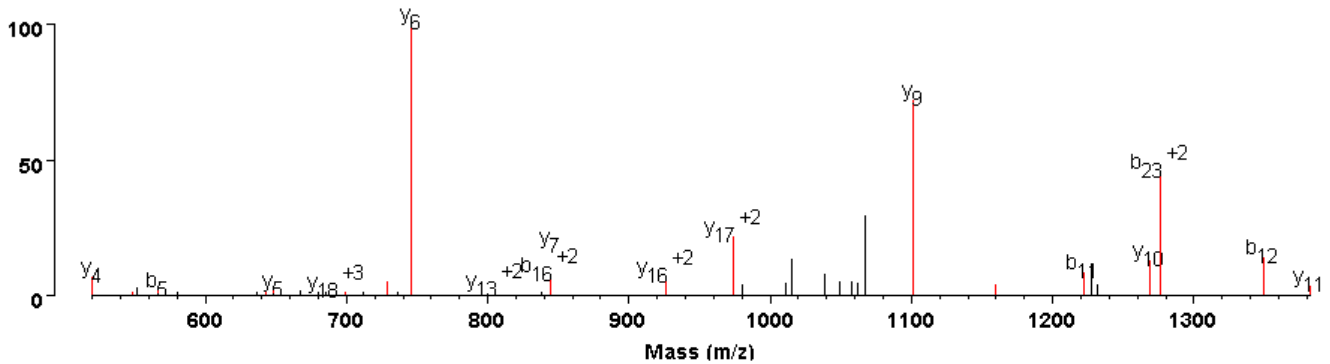

Max Intensity: 4721
Num Matched: 20/40 (50.0% unmatched) Matched Intensity: 74.7% Matched Series Intensity: 74.7%

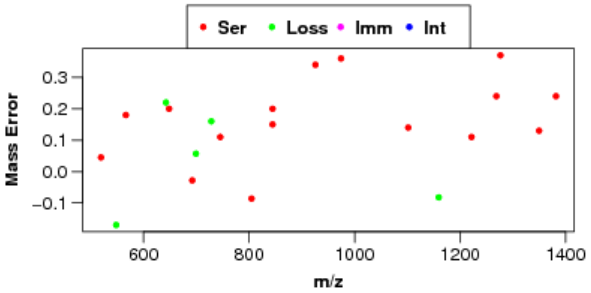

N Term	Sequence	C Term	N Loss
☑	TMVSFVSQVLEKPGLALNLS(Phospho)PC(Carbamidomethyl)VPETNER		

[+] Additional Sequences

Max Charge 3 | Count Basic AA | Max Losses 1 | Multi Z Internal ☐ | Max Internal Len 200

Max MSMS Pks | Frag Tol 0.4 Da | Cal ☐ Cal Tol (Da) 0.4

Centroid | MS-Product | Output HTML

[+] Ion Types

Elemental Composition: C140 H233 N37 O48 S2 P1

MH^{+1}(av)	MH^{+1}(mono)	MH^{+2}(av)	MH^{+2}(mono)	MH^{+3}(av)	MH^{+3}(mono)
3297.7341	3295.6102	1649.3707	1648.3088	1099.9163	1099.2083

[−] Peak Matches

519.2970	**548.0850**	**551.7210**	**566.4400**	**571.4630**	**580.4510**	**636.4670**	**642.5290**	**648.4960**	**667.4680**
y_4(0.045)	b_5-H_2O(-0.17)		b_5(0.18)				y_{11}-$H_3PO_4^{+2}$(0.22)	y_5(0.20)	
679.7140	**685.5370**	**692.3100**	**699.3850**	**711.4000**	**728.4800**	**736.5370**	**745.4600**	**804.7720**	**837.7370**
		y_{18}^{+3}(-0.028)	y_{12}-$H_3PO_4^{+2}$(0.057)		y_6-NH_3(0.16)		y_6(0.11)	y_{13}^{+2}(-0.086)	
844.6130	**925.7720**	**974.3130**	**980.6970**	**1010.7250**	**1015.0250**	**1038.4880**	**1049.6050**	**1057.7320**	**1061.4570**
b_{16}^{+2}(0.15) y_7(0.20)	y_{16}^{+2}(0.34)	y_{17}^{+2}(0.36)							
1067.2420	**1101.6400**	**1159.5300**	**1221.7250**	**1227.9750**	**1231.5260**	**1268.7340**	**1276.5090**	**1349.8410**	**1381.8250**
	y_9(0.14)	y_{21}-$H_3PO_4^{+2}$(-0.082)	b_{11}(0.11)			y_{10}(0.24)	b_{23}^{+2}(0.37)	b_{12}(0.13)	y_{11}(0.24)

b-H_3PO_4	b-$H_3PO_4^{+2}$	b	b^{+2}				y	y^{+2}	y-H_3PO_4	y-$H_3PO_4^{+2}$
---	---	---	---	1	T	29	---	---	---	---
---	---	*233.0954*	---	2	M	28	*3194.5625*	*1597.7849*	*3096.5857*	*1548.7965*
---	---	*332.1639*	---	3	V	27	*3063.5221*	*1532.2647*	*2965.5452*	*1483.2762*
---	---	*419.1959*	---	4	S	26	*2964.4536*	*1482.7305*	*2866.4768*	*1433.7420*
---	---	566.2643	---	5	F	25	*2877.4216*	*1439.2144*	*2779.4447*	*1390.2260*
---	---	665.3327	---	6	V	24	*2730.3532*	1365.6802	*2632.3763*	1316.6918
---	---	752.3647	---	7	S	23	*2631.2848*	1316.1460	*2533.3079*	1267.1576
---	---	880.4233	---	8	Q	22	*2544.2528*	1272.6300	*2446.2759*	1223.6416
---	---	979.4917	---	9	V	21	*2416.1942*	1208.6007	*2318.2173*	1159.6123
---	---	1092.5758	---	10	L	20	*2317.1258*	1159.0665	*2219.1489*	1110.0781
---	---	1221.6184	---	11	E	19	*2204.0417*	1102.5245	*2106.0648*	1053.5360
---	---	1349.7133	675.3603	12	K	18	*2074.9991*	1038.0032	*1977.0222*	989.0147
---	---	*1446.7661*	723.8867	13	P	17	*1946.9042*	973.9557	*1848.9273*	924.9673
---	---	*1503.7876*	752.3974	14	G	16	*1849.8514*	925.4293	*1751.8745*	876.4409
---	---	*1616.8716*	808.9395	15	L	15	*1792.8299*	896.9186	*1694.8530*	847.9302
---	---	*1687.9088*	844.4580	16	A	14	*1679.7459*	840.3766	*1581.7690*	791.3881
---	---	*1800.9928*	901.0000	17	L	13	*1608.7087*	804.8580	*1510.7319*	755.8696
---	---	*1915.0357*	958.0215	18	N	12	*1495.6247*	748.3160	*1397.6478*	699.3275
---	---	*2028.1198*	1014.5635	19	L	11	1381.5818	691.2945	1283.6049	642.3061
2097.1413	1049.0743	*2195.1182*	1098.0627	20	S(Phospho)	10	1268.4977	634.7525	1170.5208	585.7640
2194.1940	1097.6007	*2292.1709*	1146.5891	21	P	9	1101.4993	551.2533	---	---
2354.2247	1177.6160	*2452.2016*	1226.6044	22	C(Carbamidomethyl)	8	1004.4466	*502.7269*	---	---
2453.2931	1227.1502	*2551.2700*	1276.1386	23	V	7	844.4159	*422.7116*	---	---
2550.3459	1275.6766	*2648.3228*	1324.6650	24	P	6	745.3475	*373.1774*	---	---
2679.3885	1340.1979	*2777.3654*	*1389.1863*	25	E	5	648.2947	*324.6510*	---	---
2780.4361	*1390.7217*	*2878.4130*	*1439.7102*	26	T	4	519.2522	*260.1297*	---	---
2894.4791	*1447.7432*	*2992.4560*	*1496.7316*	27	N	3	*418.2045*	*209.6059*	---	---
3023.5217	*1512.2645*	*3121.4986*	*1561.2529*	28	E	2	*304.1615*	*152.5844*	---	---
---	---	---	---	29	R	1	*175.1190*	*88.0631*	---	---

Phospho-Thr238lSer239. Corresponding phosphopeptide represents [228-245] of HSFA4A (Uniprot ID:O49403).

TC(Carbamidomethyl)VVVREEGST(Phospho)SPSSHTR^{+3}

TC(Carbamidomethyl)VVVREEGSTS(Phospho)PSSHTR^{+3}

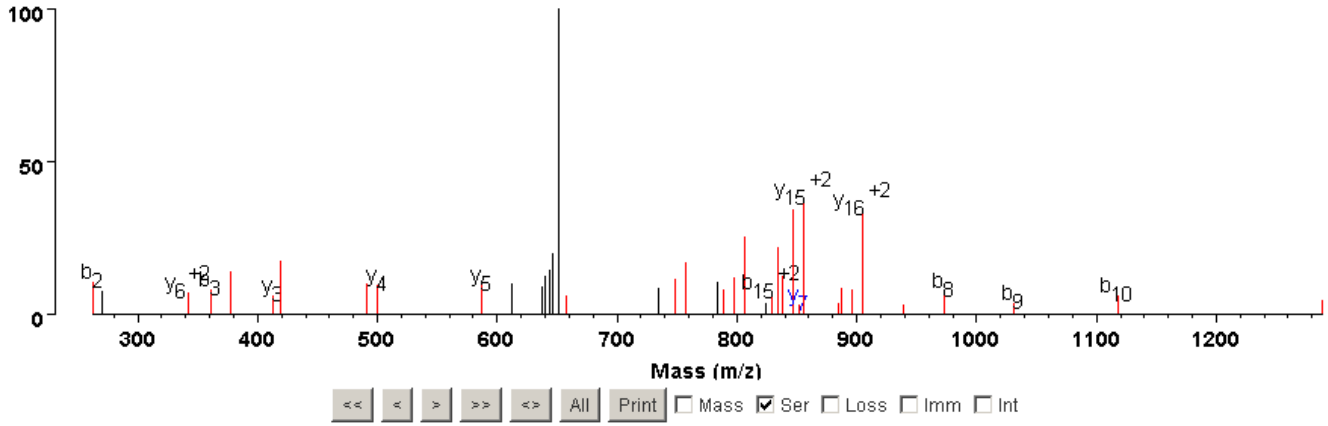

Max Intensity: 1453
Num Matched: 28/40 (30.0% unmatched) Matched Intensity: 60.9% Matched Series Intensity: 60.4%
Num Matched: 30/40 (25.0% unmatched) Matched Intensity: 65.3% Matched Series Intensity: 64.9%

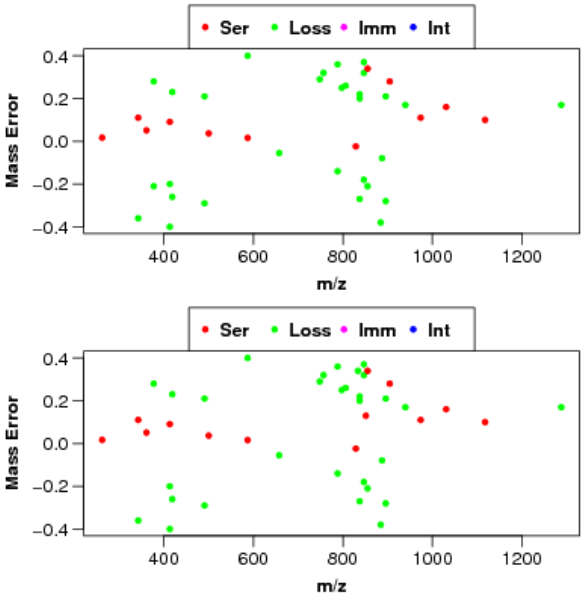

	N Term	Sequence	C Term	N Loss
☑		TC(Carbamidomethyl)VVVREEGST(Phospho)SPSSHTR		

[–] Additional Sequences

☑		TC(Carbamidomethyl)VVVREEGSTS(Phospho)PSSHTR		
☐				
☐				
☐				
☐				

Alt ☑ Discriminating ☐ Link Search Type: No Link

Max Charge: 3 | Count Basic AA | Max Losses: 2 | Multi Z Internal ☐ | Max Internal Len: 200

Max MSMS Pks | Frag Tol: 0.4 Da | Cal ☐ Cal Tol (Da): 0.4

Centroid | MS-Product | Output: HTML

[+] Ion Types

Elemental Composition: C79 H135 N27 O34 S1 P1

MH^{+1}(av)	MH^{+1}(mono)	MH^{+2}(av)	MH^{+2}(mono)	MH^{+3}(av)	MH^{+3}(mono)
2070.1520	2068.9118	1035.5797	1034.9595	690.7223	690.3088

[–] Peak Matches

262.1030	269.9970	342.7810	361.2050	377.4640	413.3170	418.9380	490.9370	500.2950	587.3060
b_2(0.017)		y_6^{+2}(0.11) b_3-H_2O(-0.36)	b_3(0.051)	y_7-NH_3^{+2}(-0.21) y_7-H_2O^{+2}(0.28) y_7-$H_3PO_4^{+2}$(0.28)	y_3(0.091) y_{12}-H_3PO_4-H_2O^{+3}(-0.20) b_7-H_2O^{+2}(-0.40)	y_8-H_3PO_4-H_2O^{+2}(0.23) y_8-H_3PO_4-NH_3^{+2}(-0.26)	y_{10}-H_3PO_4-H_2O^{+2}(0.21) y_{10}-H_3PO_4-NH_3^{+2}(-0.29)	y_4(0.037)	y_5(0.016) b_{16}-H_2O-NH_3^{+3}(0.40)
612.0490	**637.6680**	**639.8930**	**643.3510**	**645.7920**	**651.7770**	**657.5950**	**734.2330**	**748.1400**	**756.6790**
						MH-$H_3PO_4^{+3}$(-0.055)		y_{14}-H_3PO_4-NH_3^{+2}(0.29)	y_{14}-$H_3PO_4^{+2}$(0.32)
784.2730	**788.1890**	**797.6310**	**806.1590**	**824.5590**	**828.8260**	**833.6740**	**837.5860**	**846.7430**	**851.4730**
	y_{14}-$2NH_3^{+2}$(-0.14) y_{14}-H_2O-NH_3^{+2}(0.36)	y_{15}-H_3PO_4-NH_3^{+2}(0.25)	y_{15}-$H_3PO_4^{+2}$(0.26)		b_{15}^{+2}(-0.024)	y_7-H_2O(0.34)	y_8-H_3PO_4-NH_3(0.20) y_{15}-H_2O-NH_3^{+2}(0.22) y_{15}-$2NH_3^{+2}$(-0.27)	y_{16}-H_3PO_4-NH_3^{+2}(-0.18) y_{16}-H_3PO_4-H_2O^{+2}(0.32) y_{15}-NH_3^{+2}(0.37)	y_7(0.13)
855.2230	**884.5350**	**887.3150**	**895.6300**	**904.7030**	**939.5580**	**973.5860**	**1030.6550**	**1117.6350**	**1287.7680**
y_{16}-$H_3PO_4^{+2}$(-0.21) y_{15}^{+2}(0.34)	a_{17}-$H_3PO_4^{+2}$(-0.38)	y_{16}-$2NH_3^{+2}$(-0.079)	y_{16}-H_2O^{+2}(0.21) y_{16}-NH_3^{+2}(-0.28)	y_{16}^{+2}(0.28)	b_{17}-NH_3^{+2}(0.17)	b_8(0.11)	b_9(0.16)	b_{10}(0.10)	b_{12}-H_3PO_4(0.17)

[–] Main Sequence Ions

b-H_3PO_4	b-$H_3PO_4^{+2}$	b	b^{+2}				y	y^{+2}	y-H_3PO_4	y-$H_3PO_4^{+2}$
---	---	---	---	1	T	18	---	---	---	---
---	---	262.0856	---	2	C(Carbamidomethyl)	17	*1967.8641*	984.4357	*1869.8872*	935.4472
---	---	361.1540	---	3	V	16	*1807.8334*	904.4204	*1709.8565*	855.4319
---	---	460.2224	---	4	V	15	*1708.7650*	854.8861	*1610.7881*	805.8977
---	---	559.2908	---	5	V	14	*1609.6966*	805.3519	*1511.7197*	756.3635
---	---	715.3920	358.1996	6	R	13	*1510.6282*	755.8177	*1412.6513*	706.8293
---	---	844.4345	422.7209	7	E	12	*1354.5271*	677.7672	1256.5502	628.7787
---	---	973.4771	487.2422	8	E	11	1225.4845	613.2459	1127.5076	564.2574
---	---	1030.4986	515.7529	9	G	10	1096.4419	548.7246	998.4650	499.7361
---	---	1117.5306	559.2690	10	S	9	1039.4204	520.2139	941.4435	471.2254
1200.5677	600.7875	*1298.5446*	649.7760	11	T(Phospho)	8	952.3884	476.6978	854.4115	427.7094
1287.5998	644.3035	*1385.5767*	693.2920	12	S	7	771.3744	386.1908	---	---
1384.6525	692.8299	*1482.6294*	741.8184	13	P	6	684.3424	342.6748	---	---
1471.6846	736.3459	*1569.6615*	785.3344	14	S	5	587.2896	294.1484	---	---
1558.7166	779.8619	*1656.6935*	828.8504	15	S	4	500.2576	*250.6324*	---	---
1695.7755	848.3914	*1793.7524*	897.3798	16	H	3	413.2255	*207.1164*	---	---
1796.8232	898.9152	*1894.8001*	947.9037	17	T	2	276.1666	*138.5870*	---	---
---	---	---	---	18	R	1	*175.1190*	*88.0631*	---	---

Unassigned fragment ion m/z 651.8 corresponds to double neutral loss of phosphoric acid and water from the precursor peptide

Phospho-Ser309. **Corresponding phosphopeptide represents [304-311] of HSFA4A (Uniprot ID:O49403)**

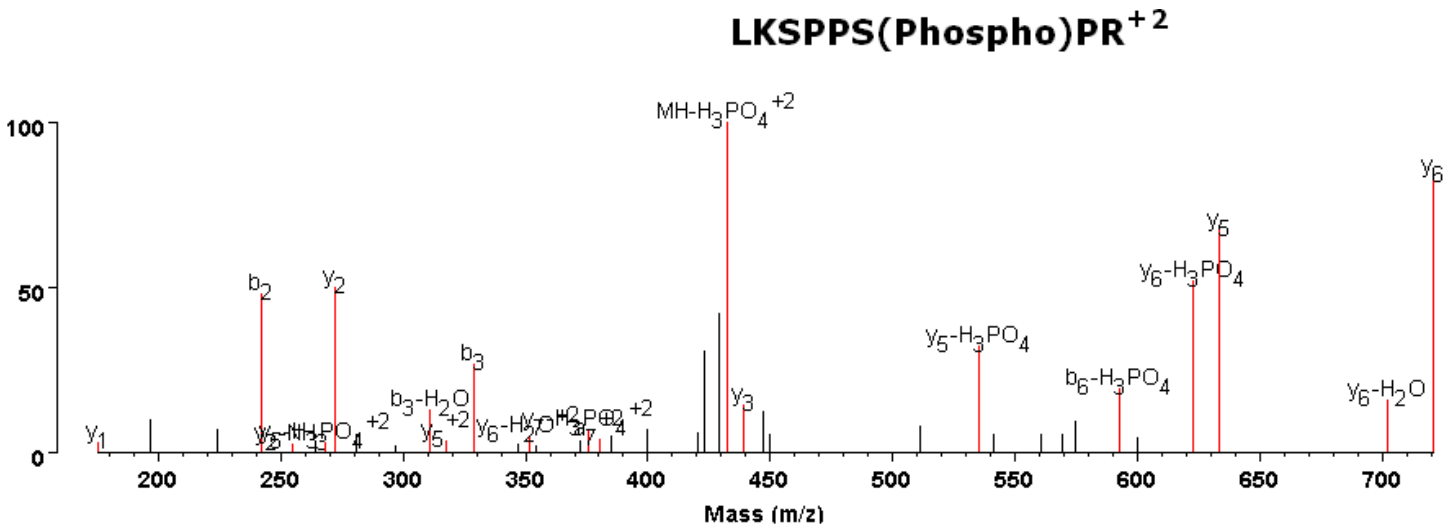

Max Intensity: 1344
Num Matched: 19/40 (52.5% unmatched) Matched Intensity: 74.7% Matched Series Intensity: 70.8%

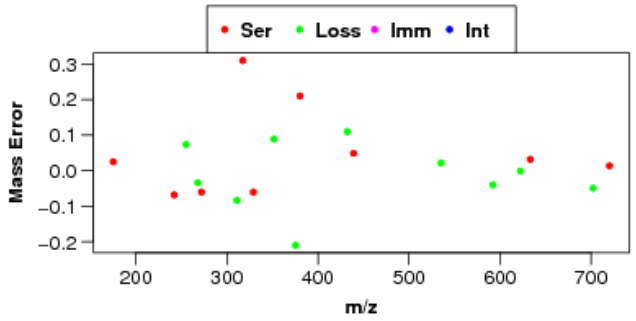

	N Term	Sequence	C Term	N Loss
☑		LKSPPS(Phospho)PR		

[+] Additional Sequences

Max Charge 2 | Count Basic AA | Max Losses 1 | Multi Z Internal ☐ | Max Internal Len 200

Max MSMS Pks | Frag Tol 0.4 Da | Cal ☐ Cal Tol (Da) 0.4

Centroid | MS-Product | Output HTML

[+] Ion Types

Elemental Composition: C39 H70 N12 O14 P1

MH^{+1}(av)	MH^{+1}(mono)	MH^{+2}(av)	MH^{+2}(mono)
962.0366	961.4867	481.5220	481.2470

[–] Peak Matches

175.1440	**197.1040**	**224.0730**	**242.1180**	**255.2190**	**264.1920**	**268.1190**	**272.1120**	**281.0620**	**297.1980**
y_1(0.025)			b_2(-0.068)	y_2-NH_3(0.074)		y_5-$H_3PO_4^{+2}$(-0.034)	y_2(-0.060)		
311.1250	**317.4550**	**329.1580**	**346.8980**	**351.7410**	**354.1840**	**372.1180**	**375.5020**	**380.4050**	**384.7750**
b_3-H_2O(-0.083)	y_5^{+2}(0.31)	b_3(-0.060)		y_6-H_2O^{+2}(0.089)			y_7-$H_3PO_4^{+2}$(-0.21)	a_7^{+2}(0.21)	
399.5220	**420.2890**	**423.3290**	**428.8630**	**432.3660**	**439.2190**	**446.9310**	**449.4720**	**511.0010**	**535.3210**
				MH-$H_3PO_4^{+2}$(0.11)	y_3(0.049)				y_5-H_3PO_4(0.022)
541.1710	**560.2280**	**568.9080**	**574.3860**	**592.3050**	**599.8280**	**622.3300**	**633.3080**	**702.2480**	**720.3220**
				b_6-H_3PO_4(-0.040)		y_6-H_3PO_4(-7.4e-4)	y_5(0.032)	y_6-H_2O(-0.049)	y_6(0.014)

[–] Main Sequence Ions

b-H_3PO_4	b-$H_3PO_4^{+2}$	b	b^{+2}				y	y^{+2}	y-H_3PO_4	y-$H_3PO_4^{+2}$
---	---	---	---	1	L	8	---	---	---	---
---	---	242.1863	*121.5968*	2	K	7	*848.4026*	424.7049	*750.4257*	375.7165
---	---	329.2183	*165.1128*	3	S	6	720.3076	360.6575	622.3307	311.6690
---	---	426.2711	213.6392	4	P	5	633.2756	317.1414	535.2987	268.1530
---	---	523.3239	262.1656	5	P	4	536.2228	268.6151	438.2459	219.6266
592.3453	296.6763	690.3222	345.6647	6	S(Phospho)	3	439.1701	220.0887	341.1932	*171.1002*
689.3981	345.2027	*787.3750*	394.1911	7	P	2	272.1717	*136.5895*	---	---
---	---	---	---	8	R	1	175.1190	*88.0631*	---	---

Phospho-Thr396. **Corresponding phosphopeptide represents [384-401] of HSFA4A (Uniprot ID:O49403)**

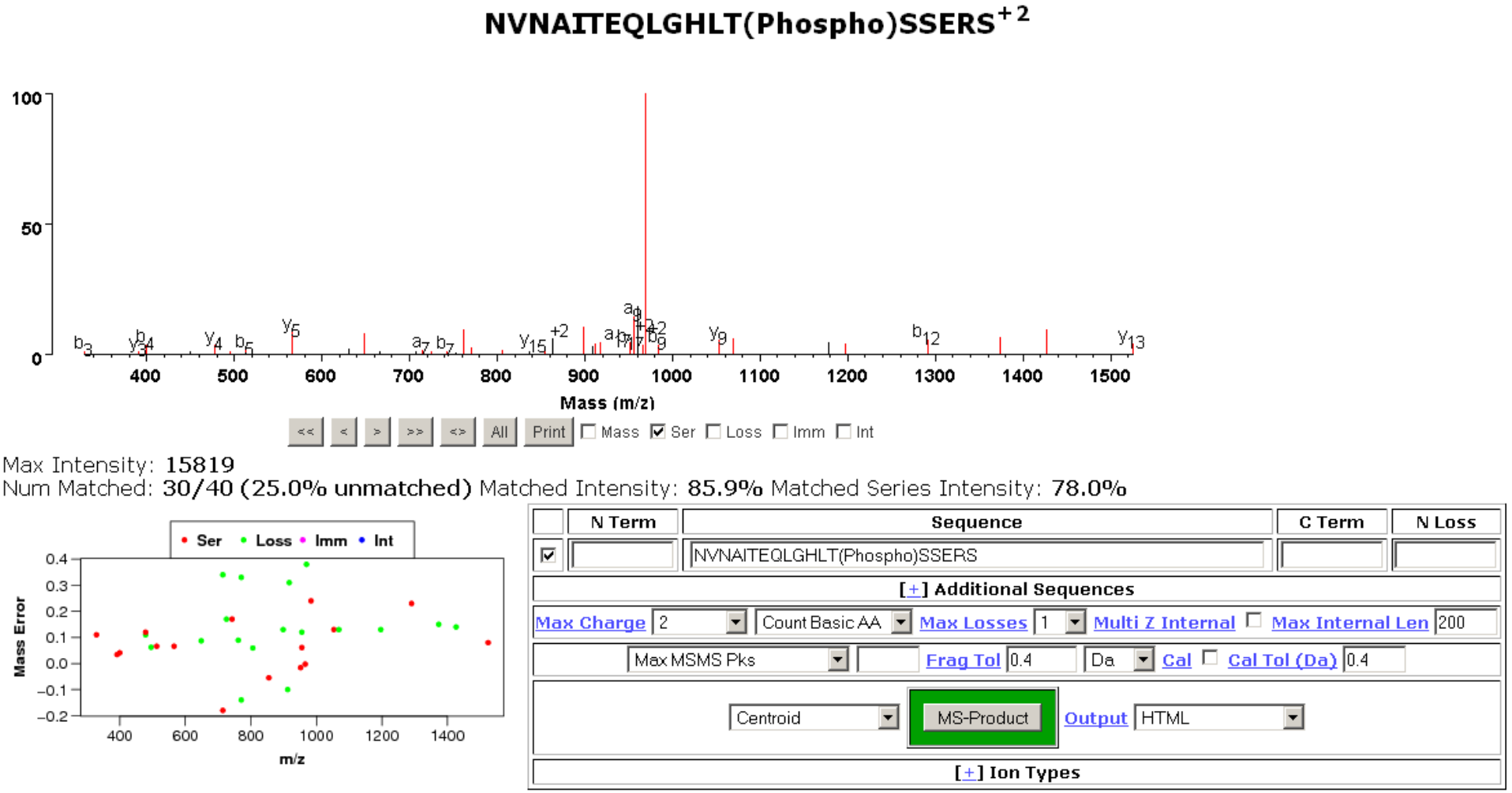

Elemental Composition: C80 H136 N26 O34 P1

MH^{+1}(av)	MH^{+1}(mono)	MH^{+2}(av)	MH^{+2}(mono)
2037.1000	2035.9444	1019.0537	1018.4759

[–] Peak Matches

328.2760	**391.2280**	**399.2400**	**450.2190**	**478.3480**	**495.3180**	**512.3490**	**565.3240**	**630.4660**	**648.3820**
b_3(0.11)	y_3(0.034)	b_4(0.041)		y_9-$H_3PO_4^{+2}$(0.11) y_4(0.12)	b_5-NH_3(0.062)	b_5(0.066)	y_5(0.066)		y_6-H_3PO_4(0.087)
666.1570	**707.5750**	**714.1940**	**725.5170**	**742.5440**	**753.3540**	**761.4680**	**770.7210**	**805.9690**	**836.4990**
		a_7(-0.18) y_{13}-$H_3PO_4^{+2}$(0.34)	b_7-NH_3(0.17)	b_7(0.17)		y_7-H_3PO_4(0.089)	b_{14}-H_2O^{+2}(-0.14) y_{14}-$H_3PO_4^{+2}$(0.33)	y_{15}-$H_3PO_4^{+2}$(0.059)	
854.8440	**863.6900**	**898.5710**	**908.8650**	**912.3660**	**917.2800**	**951.9410**	**955.5820**	**960.9070**	**965.9520**
y_{15}^{+2}(-0.055)		y_8-H_3PO_4(0.13)		y_{17}-$H_3PO_4^{+2}$(-0.100)	b_{17}-$H_3PO_4^{+2}$(0.31)	a_{17}^{+2}(-0.016)	a_9(0.061) y_9-H_3PO_4(0.12)		b_{17}^{+2}(-0.0026)
969.8710	**983.7520**	**1053.5660**	**1068.6740**	**1178.7120**	**1196.7280**	**1290.9060**	**1373.8660**	**1426.8350**	**1524.7490**
MH-$H_3PO_4^{+2}$(0.38)	b_9(0.24)	y_9(0.13)	y_{10}-H_3PO_4(0.13)		y_{11}-H_3PO_4(0.13)	b_{12}(0.23)	b_{13}-H_3PO_4(0.15)	y_{13}-H_3PO_4(0.14)	y_{13}(0.080)

[–] Main Sequence Ions

b-H_3PO_4	b-$H_3PO_4^{+2}$	b	b^{+2}				y	y^{+2}	y-H_3PO_4	y-$H_3PO_4^{+2}$
---	---	---	---	1	N	18	---	---	---	---
---	---	*214.1186*	---	2	V	17	*1921.9015*	961.4544	*1823.9246*	912.4659
---	---	328.1615	---	3	N	16	*1822.8331*	911.9202	*1724.8562*	862.9317
---	---	399.1987	---	4	A	15	*1708.7902*	854.8987	*1610.8133*	805.9103
---	---	512.2827	---	5	I	14	*1637.7531*	819.3802	*1539.7762*	770.3917
---	---	613.3304	---	6	T	13	1524.6690	762.8381	1426.6921	713.8497
---	---	742.3730	---	7	E	12	1423.6213	712.3143	1325.6444	663.3258
---	---	870.4316	---	8	Q	11	1294.5787	647.7930	1196.6018	598.8046
---	---	983.5156	---	9	L	10	1166.5201	583.7637	1068.5432	534.7753
---	---	1040.5371	---	10	G	9	1053.4361	527.2217	955.4592	478.2332
---	---	1177.5960	589.3016	11	H	8	996.4146	498.7109	898.4377	449.7225
---	---	1290.6801	645.8437	12	L	7	859.3557	430.1815	761.3788	381.1930
1373.7172	687.3622	1471.6941	736.3507	13	T(Phospho)	6	746.2716	373.6395	648.2947	*324.6510*
1460.7492	730.8782	*1558.7261*	779.8667	14	S	5	565.2576	*283.1325*	---	---
1547.7812	774.3943	*1645.7581*	823.3827	15	S	4	478.2256	*239.6164*	---	---
1676.8238	838.9156	*1774.8007*	887.9040	16	E	3	391.1936	*196.1004*	---	---
1832.9250	916.9661	*1930.9018*	965.9546	17	R	2	*262.1510*	*131.5791*	---	---
---	---	---	---	18	S	1	*106.0499*	---	---	---

Supplemental Methods

Analysis of stress tolerance

For analysis of stress tolerance traits, 5-day-old seedlings were transferred to agar-solidified 0.5 MS medium containing 5 μM estradiol and one of the following supplements: 100 mM NaCl, 5 mM H_2O_2, 0.1 mM $CdCl_2$, 0.1 or 0.3 μM paraquat. Plant growth was monitored by capturing images every 3 days as described (Ruibal, et al., 2012). Rosette size and root elongation of 30 plants were measured at each time point using the ImageJ software (rsb.info.nih.gov/ij), and average values were determined. Growth rates were calculated from at least four time points using the LINEST function of Microsoft Excel software and normalized to wild type plants.

To compare paraquat tolerance of Arabidopsis lines, seedlings were grown in the presence of 0.3 μM paraquat as indicated above. After two weeks, the anthocyanin-accumulating plants were scored, counting those seedlings that were unambiguously purple-red or showed large colored leaf sections as described by (Kortstee, et al., 2011), and percentage values were calculated.

Anoxia tolerance assay was performed on one-week-old HSFA4ox and wild type plants grown on 0.5 MS media in vertical position. Plants were sprayed with 5 μM estradiol solution and kept under high-purity nitrogen gas flow for 6 and 12 hours in a dark container. Low oxygen conditions were confirmed by testing the induction of two anaerobic marker genes *ALCOHOL DEHYDROGENASE 1* (*ADH1*, *AT1G77120*) and *PYRUVATE DECARBOXYLASE 1* (*PDC1*, *AT4G33070*) in wild type plants. Control plants (air control) were kept in the dark for 6 or 12 hours. Subsequently, plants were transferred to standard growth conditions and survival rates were scored after 7 days. All experiments were performed with two technical replicates and repeated at least 3 times.

Gene cloning, vector construction

All cloning were performed using the Gateway cloning System (Invitrogene) or FastDigest restriction enzymes and T4 DNA ligase (Thermo Scientific) following the manufacturer instructions. cDNA insert from transgenic COS lines were PCR-amplified using genomic

DNA template with the ER8A and ER8B primers (Supplemental Table 3) and Phusion High-Fidelity DNA Polymerase (Thermo Scientific). Identity of the cDNA inserts was determined by sequence homology searches in the TAIR database (www.arabidopsis.org). PCR fragments were cloned into pDONR201 using the Gateway BP clonase reaction, sequenced and moved into the binary vector pER8GW (Papdi et al., 2008) by Gateway LR clonase reaction. The *HSFA4A* (*AT4G18880*) promoter was cloned by amplifying the *HSFA4A* promoter region of 2 kb and cloning it into the pENTRY-BS vector as a *EcoRI-BamHI* fragment (pENTRY-BS vector was constructed using backbone of pENTR/D-TOPO (Invitrogene) in which MCS of pBluescript II (Stratagene) was cloned (kindly donated by T.Sarnowski, Laboratory of Plant Molecular Biology, Institute of Biochemistry and Biophysics, Polish Academy of Sciences,Warsaw). The pHSFA4A-GUS vector was generated by moving the promoter fragment into the binary vector pHGWFS7 (Karimi, et al., 2002) using Gateway LR clonase reaction.

pPCV-YFP-H vector was constructed from the modified pPCV812 vector containing the 35S promoter:mGFP4:NOS cassette (Kircher et al, 2002). The YFP cDNA was PCR-amplified from the pEYFP plasmid template (Clontech) with unique *SmaI* and *SacI* sites at the 5' and 3' termini, respectively. pPCV-YFP-H was produced by replacing the *mGFP4* gene with the amplified YFP fragment in the modified pPCV812 vector via *SmaI* and *SacI* sites. To generate the 35S-HSFA4A-YFP construct, the full-length *HSF4A4* cDNA was cloned into the expression vector pPCV-YFP-H as a *BamHI-SmaI* fragment, generating a *HSFA4A* gene 3' fusion with the YFP coding sequence.

BiFC constructs were prepared by cloning the HSFA4A cDNA into the *HindIII* and *SmaI* sites of pSAT1A-nEYFP-N1 and pSAT1A-cEYFP-N1 vectors (http://www.bio.purdue.edu/people/faculty/gelvin/nsf/index.htm). For *Agrobacterium*-mediated transient expression, BiFC constructs were subcloned as *HindIII-NotI* fragments into pENTRY-BS and moved into pH2GW7.0 and pK2GW7.0 (Karimi, et al., 2002) by LR clonase reaction.

Site directed mutagenesis of *HSFA4A* cDNA was performed using a two-step PCR amplification method as described (Brons-Poulsen, et al., 1998). To modify conserved Cys residues, a single point mutation into position C229A was introduced using a combination of HsfA4A-5'(Hind III) and 3'C229_Hsf_R primers; the resulting mega primer was used with HSFA4A-3' (SmaI)_ noSTOP primer to perform the second step PCR. The mutagenized DNA

fragment was cloned into the *HindIII* and *SmaI* sites of pENTRY-BS and sequenced. Further point mutations were consecutively introduced into positions C267A and C295A using the generated constructs as PCR templates. Finally, a PCR product containing all three point mutations in the HSFA4A coding sequence (mHSFA4A) was cloned into BiFC vectors pSAT1A-nEYFP-N1 and pSAT1A-cEYFP-N1 as a *HindIII-SmaI* fragment. To generate the mutant version Ser309HSFA4A (HSFA4m), a single point mutation was introduced in this position, and the PCR product was cloned into the *HindIII* and *SmaI* sites of pSAT1A-cEYFP-N1.

Mass Spectrometry-identified phosphorylation sites were confirmed by introducing point mutations into S198A, T238A, S239A, S309A and T396A following two-step PCR amplification method. Six individual constructs were generated and cloned into the *BamHI* and *HindIII* sites of pMAL-C2, including all combinations of quadruple point mutations and a quintuple mutant.

A PCR fragment of 1100 bp containing the promoter region of *HSP17.6A* (*AT5G12030*) was cloned into pPCV-LUC+ (Toth, et al., 2001) vector as a *EcoRI-SalI* fragment to generate the pHSP17.6A–LUC reporter gene construct.

MPK3 (*AT3G45640)* and *MPK6* (*AT2G43790)* cDNAs were PCR amplified using Arabidopsis (Col-0) cDNA as template, cloned into the bacterial expression vector pET-28c(+) (Novagen) as *BamHI-SalI* fragments and sequenced, generating the His6-MPK3/6 constructs. To generate the His6-HSFA4A construct, the corresponding cDNA was cloned into the bacterial expression vectors pET-28a(+) as *BamHI-HindIII* . MBP-HSFA4A construct was prepared cloning HSFA4A cDNA into the *BamHI* and *HindIII* sites of pMAL-C2 plasmid (NEB).

To generate yeast two hybrid constructs, MPK3, MPK6, HSFA4A and mHSFA4A coding sequences were cloned into both pGAD424 and pGBT9 vectors (Clontech) as *BamHI-SalI* fragments. To generate transgenic plants, gene constructs were introduced into Arabidopsis plants using an *in planta* transformation method (Clough, et al., 1998). Expression of inserted cDNA was tested by RT-PCR, and two overexpressing lines (HSFA4ox1 and HSFA4ox2) and one complemented mutant line (*hsfa4a*/C) were selected for further phenotypic analysis.

Analysis of gene expression

Transcript levels were monitored by real time (qRT-PCR) and semi-quantitative RT-PCR analyses. cDNA templates were generated from DNase-treated (Promega) total RNA (2 μg) samples by reverse transcription using SuperScript™ II RNase H- reverse transcriptase (Invitrogen). Real time RT-PCR reactions were prepared with SYBR® Green JumpStart™ Taq ReadyMix™ (Sigma) employing the following protocol: denaturation 95°C/10 min, 40 to 45 cycles of 95°C/10 sec and 60°C/1 min, with ABI PRISM 7700 sequence detection system (Applied Biosystems, Foster City, CA, USA). Semi-quantitative PCR reactions were performed in 50 μL volume, using 0.2 μg cDNA template and Dupla-Taq™ polymerase (Zenon Bio, Szeged) employing the following protocol: denaturation 94°C/2 min, 35 cycles of 94°C/30 sec, 60°C/45 sec, and 72°C/1 min. *TUBULIN2* (*AT5G62690*) and *GAPC2* (*AT1G13440*) genes were used as internal references. Sequences of PCR primers are listed in Table S5.

RNA-Seq Analysis

Total RNA was isolated using RNeasy kits (Qiagen). Total RNA (10 μg) was DNase I-treated with Turbo DNase (Ambion), precipitated with sodium acetate/ethanol and resuspended in nuclease-free water. RNA quality and quantity measurements were performed on Bioanalyzer (Agilent Technologies) and Qubit (Life Technologies). High quality (RIN>8.5) total RNA samples were processed using the SOLiD total RNA-Seq Kit (Life Technologies), according to the manufacturer's instructions. Briefly, 5 μg of RNA was ribosomal RNA depleted using RiboMinus Plant Kit for RNA-Seq and RiboMinus Concentration Module (both from Life Technologies). The leftover was fragmented using RNaseIII, the 50-200 nt fraction size-selected, sequencing adaptors ligated and the templates reverse transcribed using ArrayScript RT. The cDNA library was purified with Qiagen MinElute PCR Purification Kit (Qiagen) and size-selected on a 6% TBE-Urea denaturing polyacrylamide gel. The 150-250 nt cDNA fraction was amplified using AmpliTaq polymerase and purified by AmPureXP Beads (Agencourt). Concentration of each library was determined using the SOLID Library TaqMan Quantitation Kit (Life Technologies). Each library was clonally amplified on SOLiD P1 DNA Beads by emulsion PCR (ePCR). Emulsions were broken with butanol and ePCR beads enriched for template-positive beads by hybridization with magnetic enrichment beads. Template-enriched beads were extended at the 3' end in the presence of terminal transferase and 3' bead linker. Beads with the clonally amplified DNA were deposited onto SOLiD

sequencing slide and sequenced on SOLiD 5500xl Instrument using the 50-base sequencing chemistry.

Bioinformatic analysis of the RNA-Seq data was performed in colour space using Genomics Workbench 4.7.2 (CLC Bio). Raw sequencing data were trimmed by removal of low quality, short sequences so that only 50 nucleotide long sequences were used in further analysis. Sequences were mapped in a strand-specific way onto the TAIR10 version of the *A. thaliana* reference genome, using default parameters except for the following: minimum length 50%, minimum similarity 80% with the unspecific match limit set to 10. After alignment of RNA-Seq reads to the reference genome, the digital expression levels (RPKM, reads per kilobase of exon model per million mapped reads; (Mortazavi, et al., 2008) of each annotated AGI genes were calculated. To identify significantly altered gene expressions in between samples we used the RNA-Seq analysis option of the Genomics Workbench and applied Baggerley's and Kal's test with Bonferroni and FDR correction.

Mass Spectrometry

All MS data were acquired on an Orbitrap-Elite mass spectrometer (Thermo Scientific) on-line coupled to a Waters nanoAcquity HPLC. Samples were injected onto a trapping column (Waters Symmetry C18, 0.180mm ID*20mm length, 5µm particle size) with 3% solvent B at 10 µl/min than were transferred onto the separating column (Waters BEH300 C18, 0.075 mm ID*150 mm length, 1.75 µm particle size) using a linear gradient of 10-40% solvent B in 30 min at 400 nl/min. Solvent A: 0.1% formic acid / water, solvent B: 0.1% formic acid / acetonitrile. MS data acquisition was carried out in data-dependent fashion, precursor masses were measured in the Orbitrap; sequential CID and HCD spectra were acquired from the computer-selected 3 most abundant multiply charged precursor ions. CID experiments were performed with wideband activation, and the fragments were measured in the linear ion trap. HCD activation was carried out applying stepped normalized collision energy of 18% and 30%, and the fragments were measured in the Orbitrap (Medzihradszky, et al., 2009). Dynamic exclusion was enabled (mass width: ± 5 ppm), exclusion time: 60 s.

Peak picking was carried out by the PAVA software (Guan et al., 2011) and the resulting data were searched with Protein Prospector search engine (v.5.10.9.) and the resulting data were searched with Protein Prospector search engine (v.5.10.9.) using the

following parameters: database: Swissprot (2012.03.21. version, 535248 entries searched); enzyme:trypsin with maximum 1 missed cleavage site; fixed modifications: carbamidomethyl (Cys); variable modifications: acetyl (protein N-term), Gln->pyro-Glu (N-term Gln),oxidation (Met); mass accuracy: ±5 ppm for precursors and ±0.4 Da and ±10 ppm for fragment ions for CID and HCD, respectively; instrument type: ESI-TRAP for CID and Q-TOF for HCD data. As acceptance criteria we used the following settings: score=22 and 15; E value= 0.01 and 0.05 for protein and peptide identifications, respectively and SLIP score (as measure of site assignment reliability was set to the 95% cut-off value, i.e. to 6 (Baker et al., 2011). After confidently identifying the protein of interest in the nonenriched samples, database search was repeated on the sequence of the MBP-HSFA4A fusion protein allowing phosphorylation on Ser/Thr/Tyr as variable modification (max. 4 variable modifications/peptide) and maximum 2 missed cleavages. Peptide fragments are labeled according to the established nomenclature (Biemann, 1990).

Supplemental References

Baker PR, Trinidad JC, Chalkley RJ (2011) Modification site localization scoring integrated into a search engine. Mol Cell Proteomics **10:** M111 008078

Biemann K (1990) Appendix 5. Nomenclature for peptide fragment ions (positive ions). Methods Enzymol **193:** 886-887

Brons-Poulsen J, Petersen NE, Horder M, Kristiansen K (1998) An improved PCR-based method for site directed mutagenesis using megaprimers. Mol Cell Probes **12:** 345-348

Clough SJ, Bent AF (1998) Floral dip: a simplified method for *Agrobacterium*-mediated transformation of Arabidopsis thaliana. Plant J **16:** 735-743

Guan S, Price JC, Prusiner SB, Ghaemmaghami S, Burlingame AL (2011) A data processing pipeline for mammalian proteome dynamics studies using stable isotope metabolic labeling. Mol Cell Proteomics **10:** M111 010728

Karimi M, Inze D, Depicker A (2002) GATEWAY vectors for *Agrobacterium*-mediated plant transformation. Trends Plant Sci **7:** 193-195

Kircher S, Gil P, Kozma-Bognar L, Fejes E, Speth V, Husselstein-Muller T, Bauer D, Adam E, Schafer E, Nagy F (2002) Nucleocytoplasmic partitioning of the plant photoreceptors phytochrome A, B, C, D, and E is regulated differentially by light and exhibits a diurnal rhythm. Plant Cell **14:** 1541-1555

Kortstee AJ, Khan SA, Helderman C, Trindade LM, Wu Y, Visser RG, Brendolise C, Allan A, Schouten HJ, Jacobsen E (2011) Anthocyanin production as a potential visual selection marker during plant transformation. Transgenic Res **20:** 1253-1264

Medzihradszky, K. F., Chalkley, R. J., Trinidad, J. C., Michaelevski, A., and Burlingame, A. L. (2008) The utilization of Orbitrap higher collision decomposition device for PTM analysis and iTRAQ-based quantitation. 56th ASMS Conference on Mass Spectrometry, Denver, CO.USA.

Mortazavi A, Williams BA, McCue K, Schaeffer L, Wold B (2008) Mapping and quantifying mammalian transcriptomes by RNA-Seq. Nat Methods **5:** 621-628

Papdi C, Abraham E, Joseph MP, Popescu C, Koncz C, Szabados L (2008) Functional identification of Arabidopsis stress regulatory genes using the controlled cDNA overexpression system. Plant Physiol **147:** 528-542

Ruibal C, Salamo IP, Carballo V, Castro A, Bentancor M, Borsani O, Szabados L, Vidal S (2012) Differential contribution of individual dehydrin genes from Physcomitrella patens to salt and osmotic stress tolerance. Plant Sci **190:** 89-102

Toth R, Kevei E, Hall A, Millar AJ, Nagy F, Kozma-Bognar L (2001) Circadian clock-regulated expression of phytochrome and cryptochrome genes in Arabidopsis. Plant Physiol **127:** 1607-1616

van Dongen JT, Roeb GW, Dautzenberg M, Froehlich A, Vigeolas H, Minchin PE, Geigenberger P (2004) Phloem import and storage metabolism are highly coordinated by the low oxygen concentrations within developing wheat seeds. Plant Physiol **135:** 1809-1821